

# An Analysis of the Inmarsat Data from MH370

Dr Richard E Cole University College London

16/6/14 issue 1

## Summary:

The detailed analysis of the Inmarsat communications data used in the search for Flight MH370 has not been released to the Public. This paper describes a model for interpreting the Inmarsat Doppler or BFO data which has been developed using the published 'raw' Inmarsat data and basic model plus other information in the public domain. The model requires only minor adjustments for frequency drift to predict final search areas consistent with those declared by the official investigation. Without access to the data from other flights a full verification of this model is not possible. However, based on the information available no major discrepancies in the BFO analysis performed by the official investigation have been identified.

## Contents

1	Introduction.....	2
2	The Inmarsat Data .....	2
3	The BTO (Ping-Arc) Model .....	3
4	The BFO (Doppler) Model.....	5
5	Radar Data .....	12
6	The Track Model .....	13
7	Results of using the BTO and BFO data with the Track Model.....	14
8	Levels of statistical confidence .....	26
9	Conclusions.....	27
10	References .....	27

### List of Appendices:

- A List of acronyms
- B Ping Arcs distances derived from the BTO measurements
- C Determination of the term D3satellite → ground
- D Determination of the constant D5offset
- E Description of the statistical tests used for BFO data
- F Plots of the components of the Refined BFO Model
- G Wind data

# 1 Introduction

Contact was lost with Malaysian Airlines flight MH370 at around 17:20UT on the 7<sup>th</sup> March 2014. Despite extensive searches no trace has been found three months later. During March 2014 the Inmarsat company released limited information regarding communications between MH370 and their satellite system [2]. It was stated that the aircraft had remained airborne for many hours after radio contact was lost and had travelled distances of thousands of kilometres. Later in March 2014 Inmarsat and others released the conclusion that the aircraft had travelled South to a point in the Southern Ocean or South Indian Ocean. The original Inmarsat communication log was released at the end of May 2014 [1]. However, the full analysis has not been presented by the Malaysian authorities on the stated basis that the information is confidential to the continuing investigation. This has resulted in speculation over the data analysis process that has been followed.

The purpose of this paper is to present an independent analysis of the satellite communications data (including the so-called pings) to assist in understanding the process followed by the investigation in reaching their published conclusions. The paper is not intended to criticise the investigation or to offer an alternative solution for the final location of MH370.

The analysis is based on the Inmarsat data and the reported turn-back point of MH370 at 17:21 on 7<sup>th</sup> March 2014. No other position data reported at the time is used, but a comparison with the radar data on unidentified targets near Malaysia is offered.

The information used is that released by Inmarsat and the Malaysian authorities together with other data available in the public domain. No confidential information has been used.

In the text the original sources are referenced in square brackets and listed at the end of the paper. Text quoted from original documents is shown in italics.

## 2 The Inmarsat Data

### 2.1 *The Data*

The Inmarsat raw data was released on 27<sup>th</sup> May together with limited explanatory notes [1]. This was stated to be the logs from the ground station before any data processing specific to the MH370 situation – it is the routine data stored for all communications in the Inmarsat system. The data includes the following key parameters:

Burst Timing Offset (BTO): A measure of the total time for radio signals to travel from the Inmarsat control centre via the satellite to the aircraft and back. The BTO is given in microseconds.

Burst Frequency Offset (BFO): A measure of the frequency offset of the radio signal received at the Inmarsat ground station from the expected value. The BFO is given in Hertz (Hz).

These data are stated by Inmarsat to be adequate to derive the geographical position of the aircraft between 17:21UT on the 7<sup>th</sup> March and 00:19UT on the 8<sup>th</sup> March.

The models used by Inmarsat and other agencies to analyse the data were not released, beyond the outline published on 25/3/14 [2].

## 2.2 The Satellite System

This paper does not attempt to give an end-to-end description of the Inmarsat 3F1 satellite or its Inmarsat-C communications payload. Details of the latter are given in an application to the US FCC for the Inmarsat 3F3 satellite [3] which is believed to be very similar or identical to Inmarsat 3F1. Details of the Inmarsat control system for the Inmarsat-3 series were published some years ago [6].

The information that is relevant to this paper is as follows:

1. Inmarsat 3F1 satellite is in a near Geostationary Orbit with an inclination of 1.67degrees. The orbit has a small eccentricity which affects its distance from the Earth by a few kilometres over each orbit.
2. The Inmarsat-C communications payload communicates with the Land, Maritime and Aeronautical terminals at L-band frequencies (1 to 2 GHz) and with the ground station at C-band frequencies (roughly 4–8 GHz). The payload acts as a ‘bent-pipe’, receiving and re-transmitting the signals received without decoding them to digital form – it does not ‘read’ the data.
3. The precise communication frequency used for the return path from the satellite terminal on MH370 and to the ground station at Perth were 1.6GHz and 3.6GHz respectively.
4. The communications data is transferred at C-band to the Perth ground station at 31°48’21”S, 115°53’16”E. The satellite is controlled by the Fucino ground station at 41°58’44”N, 13°36’7”E.

Orbital elements for the Inmarsat 3F1 satellite for the period including 7<sup>th</sup> March 2014 were obtained from public sources. The satellite’s position in space and its spatial relationships to the ground stations were obtained using Orbitron, a simple orbital analysis tool with which the Author was familiar. Comparisons with data published by others using the industry standard STK package did not reveal any discrepancies.

## 3 The BTO (Ping-Arc) Model

The BTO values are related to the time taken for the radio signals to travel from the ground to the satellite, then to the aircraft and then back again to the satellite and ground station. However, it is not that total time for that trip (which would be much longer than the BTO numbers in the log) but some parameter derived from it. The Inmarsat notes state:

- *The round trip time for a message is a combination of:*
  1. *Time from the ground station → satellite → aircraft → satellite ground station*
  2. *Processing time within the ground station, satellite and aircraft terminal, which are constant*
- *The BTO is a value (in microseconds) relative to a terminal at a nominal fixed location. Only R-Channel messages are used.*

The nominal fixed terminal (hereafter the nominal terminal) is a ‘virtual’ terminal which exists only in the Inmarsat processing system to allow them to log (in real-time) some meaningful (and short) numbers. The BTO is the time for signals to travel from the ground station to the aircraft via the satellite and back with respect to the time taken to travel to the nominal terminal via the satellite, and back. This definition removes the time taken for signals to travel from ground station to the satellite. A schematic of the Nominal Terminal concept is shown in Figure 1. The simplest assumption is the Nominal Terminal is set at a

fixed altitude above the equator at longitude 64.5E. Thus the length of the green line segment in Figure 1 is the distance determined by the individual BTO values.

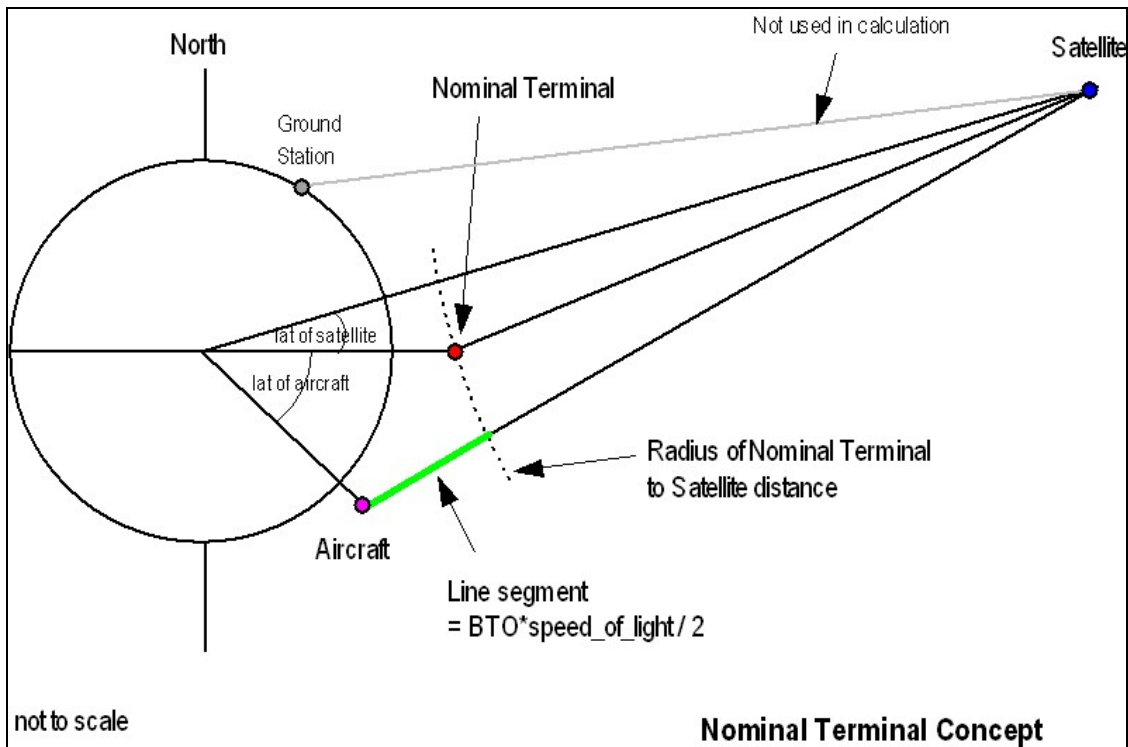


**Figure 1: Nominal Terminal concept used for analysis of the BTO data**

The distance of the Nominal Terminal from the satellite can be calculated from the BTO measurements when MH370 was on the ground at Kuala Lumpur airport and thus when its exact position was known. The ‘virtual’ altitude of the Nominal Terminal was calculated to be 718km. With the Nominal Terminal position fixed with respect to the Earth, the later BTO values can be translated into the distance of MH370 from the Inmarsat 3F1 satellite and hence a circle on the ground for each BTO measurement. The position of the satellite at the time of each BTO measurement is required and be derived from the orbital elements. These circles are the ping rings. Their precise geographical positions depend on the height of the aircraft above the ground which cannot be derived from the data, but this affects the radii of the ping rings by only up to 7km.

The ping rings derived by this technique match the graph of satellite elevation shown to the MH370 families at a briefing but only available as a fuzzy photograph – the data was not formally released otherwise. Hereafter the ping-rings used are derived using the technique above and are listed in Appendix B.

## 4 The BFO (Doppler) Model

### 4.1 Background

The investigation published an outline of the BFO model on 25/3/14 [2]. This stated that the Total Doppler shift on the communications link between the aircraft and the Inmarsat satellite could be represented as:

$$Total \_ Doppler = D1_{aircraft} + D2_{aircraft \rightarrow satellite} + D3_{satellite \rightarrow ground} \quad \text{equation 1}$$

The burst frequency offset is the difference (due to the Doppler contributions) between the expected received frequency and that actually measured.

$D2$  is a combination of the Doppler components due to the satellite motion, which is accurately known, and the aircraft heading and speed. Using the burst frequency offsets measured at the land earth station, it is possible to compare against the predictions for aircraft heading and speed.

$[D2_{aircraft \rightarrow satellite}]$  not corrected by system = measured frequency offset.

This concept is shown in Figure 2 taken from [2].

The work presented here works from this basis and proceeds to break down the model further. An explanation of each component of the model is offered.

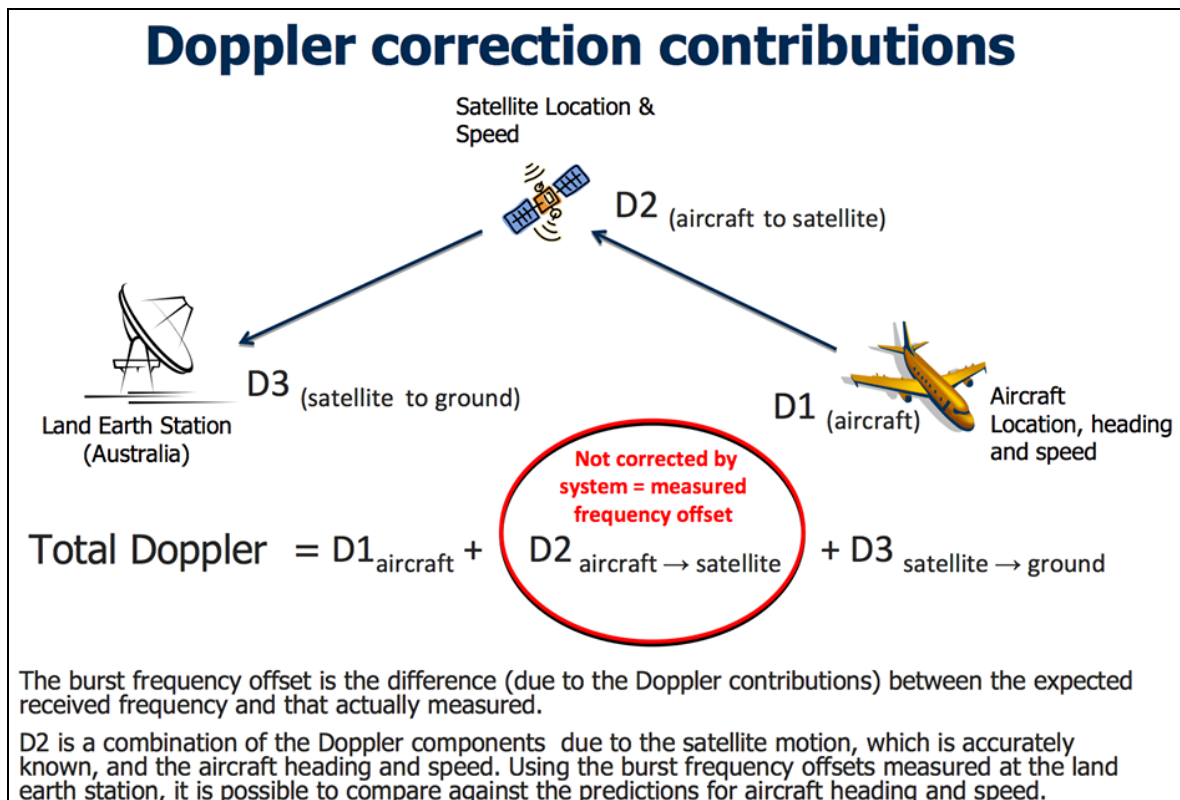


Figure 2: Original diagram released on 25/3/14 to explain the Doppler/BFO concept [2]

## 4.2 The refined BFO Model

The BFO model discussed here can be stated as follows (equation 2):

$$BFO = D1_{aircraft} + D2_{aircraft} + D2_{satellite} + D3_{satellite \rightarrow ground} + D4_{drift} + D5_{offset} \quad \text{equation 2}$$

The nomenclature of the original publication [2] is retained as far as possible, though a number of the terms in the refined BFO model are not the result of the Doppler Effect (as might be implied by the letter ‘D’). The components are summarised in Table 1 and described in more detail in the following sections.

Element	Summary
D1 <sub>aircraft</sub>	The correction applied to the return L-band transmission frequency by the satellite terminal in the aircraft. This is calculated inside the terminal in real-time.
D2 <sub>aircraft</sub>	The Doppler shift in the return L-band transmission from the aircraft to the satellite due to the velocity of the aircraft. It is a function of the aircraft’s speed, course, rate of change of altitude and position, and the position of the satellite.
D2 <sub>satellite</sub>	The Doppler shift in the return L-band transmission from the aircraft to the satellite due to the velocity of the Inmarsat 3F1 satellite. It is a function of the aircraft’s position and the known position and velocity of the satellite.
D3 <sub>satellite→ground</sub>	The Doppler shift in the transmissions between the satellite and the Inmarsat ground stations due to the velocity of the Inmarsat 3F1 satellite. This includes the C-band downlink to the Perth ground station and an uplink transmission from the Fucino ground station to the satellite. All the inputs to this element are known.
D4 <sub>drift</sub>	The drift of radio frequency standards in the aircraft and satellite terminals during the flight.
D5 <sub>offset</sub>	A constant offset (unchanging with time) between the model and the BFO measurements due to various factors. The value of this constant can be derived from the BFO data when the aircraft was on the ground.

**Table 1: Description of BFO model components**

## 4.3 Aircraft Terminal Correction - D1<sub>aircraft</sub>

The Inmarsat notes [1] state:

*Inmarsat Classic Aero mobile terminals are designed to correct for aircraft Doppler effects on their transmit signals. The terminal type used on MH370 assumes a stationary satellite at a fixed orbital position*

The type of terminal on MH370 is not published, but the manual for a typical Honeywell terminal (type MCS-4200/7200) [4] states (pages 1-22 and A-26):

*The SDU can adjust the transmission frequency in one—Hertz increments to compensate for the Doppler shift caused by the speed of the aircraft...*

*...If the aircraft does not have an IRS [Internal Reference System] that supplies this ARINC [Navigation] data, the SCU [Signal Conditioning Unit] can be used to supply the data.*

Thus the terminal receives position information either from the aircraft's navigation system or from its own GPS system and uses that to calculate the component of the aircraft's velocity towards the satellite. It then calculates the Doppler shift corresponding to that velocity and corrects the frequency of its L-band uplink so that the signal is received at the satellite at the correct frequency. However, the terminal uses a fixed position for the Inmarsat 3F1 satellite in this calculation [1], that is, it is assumed to be in a 'perfect' geostationary orbit at the 64.5°E orbital station. In reality the satellite is not in a fully geostationary orbit and drifts 1.6degrees North and South of the Equator (it also changes in distance from the Earth by +/- 23km, but this is a minor effect). If the terminal used the full-precision position of the satellite then component  $D1_{aircraft}$  would fully compensate for component  $D2_{aircraft}$ . However, as a result of use of a fixed satellite position in the calculation the two components are not of equal and opposite value and the difference appears in the final measured BFO. This difference is most significant when the spacecraft is at or close to its extreme North and South positions (which was the case for the early parts of the flight) and very small when the spacecraft is close to the fixed position used in the calculation (which was the case at the end of the flight). The difference is also a strong function of the heading of the aircraft, particularly when the heading is roughly towards (or away from) the position 64.5E, 0N. This effect is one of the major asymmetries between possible Northerly and Southerly tracks.

A predicted value of  $D1_{aircraft}$  can be calculated for any modelled aircraft position, speed and course, for a given time. The L-band link frequency used is 1.6GHz (see section 2.2). Data from early parts of the flight indicates that the terminal does not compensate for the vertical speed of the aircraft.

#### ***4.4 Aircraft Velocity Doppler – $D2_{aircraft}$***

This contribution is the simple Doppler frequency offset in the return L-band link between the aircraft and the satellite due to the velocity of aircraft. A predicted value of  $D2_{aircraft}$  can be calculated for any modelled aircraft position, speed, course and rate of climb/descent for a given time, using the known position of the satellite for that time. The same L-band link frequency is used as for  $D1_{aircraft}$ .

#### ***4.5 Satellite Velocity Doppler – $D2_{satellite}$***

This contribution is the simple Doppler frequency offset in the return L-band link between the aircraft and the satellite due to the velocity of satellite. A predicted value of  $D2_{aircraft}$  can be calculated for any modelled aircraft position for a given time, using the known position of the satellite for that time. The same L-band link frequency is used as for  $D2_{aircraft}$ .

#### ***4.6 Ground Station Contributions – $D3_{satellite \rightarrow ground}$***

This contribution is related to the frequency shift in the return C-band transmission from the satellite to the Inmarsat Perth ground station due to the velocity of the Inmarsat 3F1 satellite. This has a large value and

has to be fully understood before the full BFO can be evaluated correctly. It is independent of any parameter related to the aircraft, so should be completely determinable for any time since the satellite position is known. It is certainly the case that it cannot be the full Doppler shift due to the velocity of the satellite towards or away from the Perth ground station – the BFO data is just not consistent with that by around 50Hz over the period of the flight, a very large difference.

The Inmarsat notes [1] do not give a full explanation for this component but include the cryptic comment:

*The correction applied by the Automatic Frequency Control (AFC) system in the ground station partially compensates for the satellite to ground station Doppler*

It is believed that the AFC (Automatic Frequency Control) system used by the Inmarsat system is as described in the MITEQ technical note 25T020 ‘Enhanced Automatic Frequency Control for Inmarsat Earth Stations’ [5]. The description below is the best proposal for how this AFC system determines the D3 component and is consistent with the measured BFO data as is shown later.

The purpose of the AFC is to detect and correct for Doppler shifts on radio links between the spacecraft and the ground. The system as described in [5] is shown in Figure 3, extracted from that document. The Inmarsat 3F1 satellite is controlled by the Fucino ground station in Italy (the so-called TT&C station [6]). This is the Primary Earth station shown in Figure 3. The Perth Ground Station is the secondary ground station. A very well-determined ‘pilot-frequency’ is used to allow measurement of the Doppler shift on the downlink from the spacecraft to the secondary ground station – this is the C-band link carrying the aircraft communications data being analysed here.

The Pilot Frequency for the C-band downlink could in principle be generated in the satellite but in the system design chosen (Figure 3) it is generated at the primary ground station (at Fucino) at an L band frequency. This is received on board the satellite with a Doppler shift  $D_P$  determined by the velocity of the satellite with respect to Fucino.  $D_P$  can be measured at the satellite since the pilot frequency is known.

The pilot frequency is upshifted to C-band by the satellite and transmitted to Perth. This is received at Perth with an additional Doppler shift  $D_S$  due to the (different) velocity of the satellite with respect to Perth. So the total Doppler shift of the pilot frequency at Perth is  $D_T$ :

$$D_T = D_P + D_S \qquad \text{equation 3}$$

Examination of the BFO data indicates that component  $D_{3\text{satellite} \rightarrow \text{ground}}$  is equal to  $D_T$ , not  $D_S$ . The documentation does not indicate why this should be so, but it is possible that the return L-band transmissions from the Land and Aircraft stations are upshifted to C-band on the satellite by an amount adjusted for the value of  $D_P$ . This would allow the downlink pilot frequency (received from Fucino and re-transmitted at C-band) to be included in that downlink at a position related to its correct frequency as generated at the Primary Earth station. Otherwise it would change position as the value of  $D_P$  varies due to the changing position of the satellite with respect to Fucino.

As Fucino is in the Northern hemisphere and Perth in the Southern,  $D_P$  and  $D_S$  have opposite signs and partially cancel, so meets the Inmarsat statement that the AFC system ‘partially compensates’ for the satellite to ground station Doppler. The components of  $D_{3\text{satellite} \rightarrow \text{ground}}$  are shown in appendix C.



This description of  $D3_{\text{satellite} \rightarrow \text{ground}}$  is used in the analysis presented in this paper. If it were incorrect no match to the data would be found as the component is large (up to +/-60Hz) and thus any error would also be large. Resolving the nature of this component was vital to presenting any useful analysis.

(note: the L-band link between the satellite and the aircraft uses the velocity correction system described in section 4.3 as an alternative to AFC, so this system description is not relevant to that link)

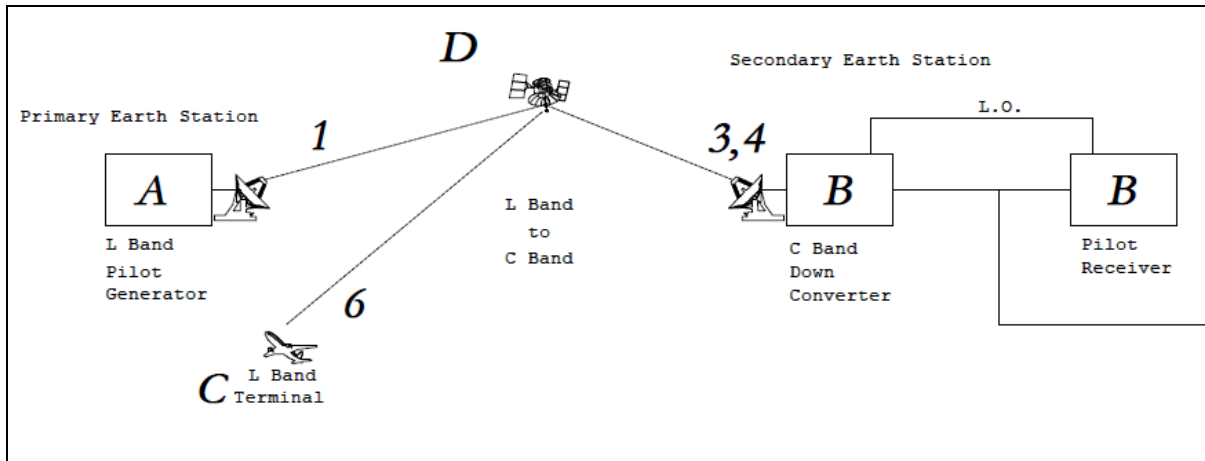


**Figure 3: AFC system believed to be used on Inmarsat 3F1, from [5]**

#### 4.7 Frequency Drift - $D4_{\text{drift}}$

The Inmarsat notes refer to ‘*Satellite, terminal and ground station oscillator stability*’. This contribution is the collection of changes in oscillator frequencies over the time of flight. All these oscillators are designed to have very high stability, so the expected changes over 6 hours should be small. However, the drifts cannot be deduced from the BFO data and require calibration of some type. It has been stated that Inmarsat had records of previous flights of the B777 9M-MRO so the stability of that system could be determined. The ground station and satellite systems are still available and calibrations were possible after 7<sup>th</sup> March.

A press report [7] indicated a concern that changes in the satellite temperature could influence the onboard oscillator frequencies (the language in the article is rather confused). The satellite was in eclipse (night) from 19:22 to 20:22UT a period which includes the 19:41UT ping. Onboard temperatures and supply voltages would change during the eclipse and for a period thereafter. The analysis later in this paper potentially indicates a larger error for the 19:41UT ping than the other pings which could indicate why the Inmarsat analysis team were concerned with this effect.

Apart from this possible eclipse effect, the sum of the drift terms could be expected to be small. However, the value cannot be determined without the calibration data which has not been released. However, the comparison with the BFO data and the final selected search areas based on the calibrated model (see later sections) suggests  $D4_{\text{drift}}$  is less than 3Hz at all times during the flight.

## 4.8 Constant Offset – $D5_{offset}$

There are a number of constant terms, for example:

1. As stated in the Inmarsat notes ‘An individual aircraft terminal will have a fixed frequency bias’
2. A positive offset will have been added by the Inmarsat system to avoid logging negative numbers (as in the case for the logged BTO numbers using the nominal terminal concept).

The sum of these constant terms can be calculated when the aircraft is stationary at KL airport at a determined position. The BFO data points before 18:30UT were examined against the expected trends of  $D2_{satellite}$  and  $D3_{satellite \rightarrow ground}$  which are changing at this time, while  $D1_{aircraft}$  and  $D2_{aircraft}$  are both zero as the aircraft is stationary. The data are shown plotted in Appendix D. A value for  $D5_{offset}$  of 151.5Hz (+/- 0.5Hz) was determined.

## 4.9 Analysis of the noise on the data

The logged values of the BFO will be not be perfect measurements, but will be subject to various sources of noise. The first source is random noise due to small errors in the signal detection and measurement chain from second to second. The logged BFO values before and after take-off were examined to understand this source of noise.

Before take-off: After exclusion of the BFO values before 16.30UT that are changing significantly (presumably due to activity in the terminal), there are periods of relative stability in the logged values. Taking the standard deviation of the BFO values in each period and then averaging those ‘averages’ gives a one sigma error of 1.6Hz.

After take-off: There is short-period at 17:07UT when the aircraft is reported in level flight. The standard deviation of the eight R-channel BFO data points at this time is 1.13Hz.

The worst of the two figures is taken for the random element of the BFO noise, so 1.6Hz.

There is also the possibility of systematic noise in the data during flight. Systematic noise is a major source of potential bias. Potential sources of such noise are:

- a. Rate of climb/descent: A rate of climb/descent rate of 50ft/min even for a very short period while the ping was being sent could significantly perturb the BFO measurement.
- b. Changes of course from those in the Track Model. A sinusoidal element to the heading of +/-7degrees could add 1Hz to individual BFO measurements.
- c. Short-term variations in RF oscillator frequency: Long-term variations are included in the model but short-term variations are unknown.

Total noise: A full treatment of noise is not possible without a full system analysis, but the major contributors may be a) the random element (1.6Hz) and b) the rate of climb/descent at the ping time. In the absence of better information a contribution from climb/descent rates of 50ft/min is assumed, an error of ~1.4Hz. These two errors are uncorrelated and therefore add in quadrature to give a value of 2.1Hz for the total error.

This will not be the correct figure for the error - a lot more work would be needed to give a full appreciation of the BFO error – but is used for the analysis in this paper.

#### 4.10 Aircraft Performance Issues

This paper does not attempt to derive constraints on the aircraft performance in which the author is not competent. The obvious issues that will constrain the conclusions of the model are:

1. The minimum speed at which the aircraft could travel. A simple search of bulletin boards suggest a B777 has a minimum clean speed of 270-280KIAS at maximum take-off weight (MTOW). The aircraft was much below MTOW at the end of the flight, but the Track Model will assume constant speed for a large part of the flight so the weight near the start of the flight would provide a constraint. True airspeed (TAS) would be higher than that figure give altitude correction, but since the altitude is not known, a TAS minimum figure of 280kt has been assumed. Clearly, the investigators would have a much better idea from a detailed aircraft analysis.
2. The maximum TAS has been taken as 500kt. There have been statements from the investigators that fuel burn rate at higher airspeeds would not allow an endurance to 00:18UT. This is discussed later in the paper.

#### 4.11 Verification of the Model

It has been stated that the model used in the investigation has been tested against flights of other aircraft and earlier flights of 9M-MRO. That data is not publically available so the only verification source are the data logs themselves plus the recorded ADS-B transmissions [11]. The BFO data and the values of BFO predicted by the Refined BFO model in the period of the flight before 17:22UT are shown in Figure 4. The position, speed, heading and rate of climb of the aircraft reported in the ADS-B data are input into the model.

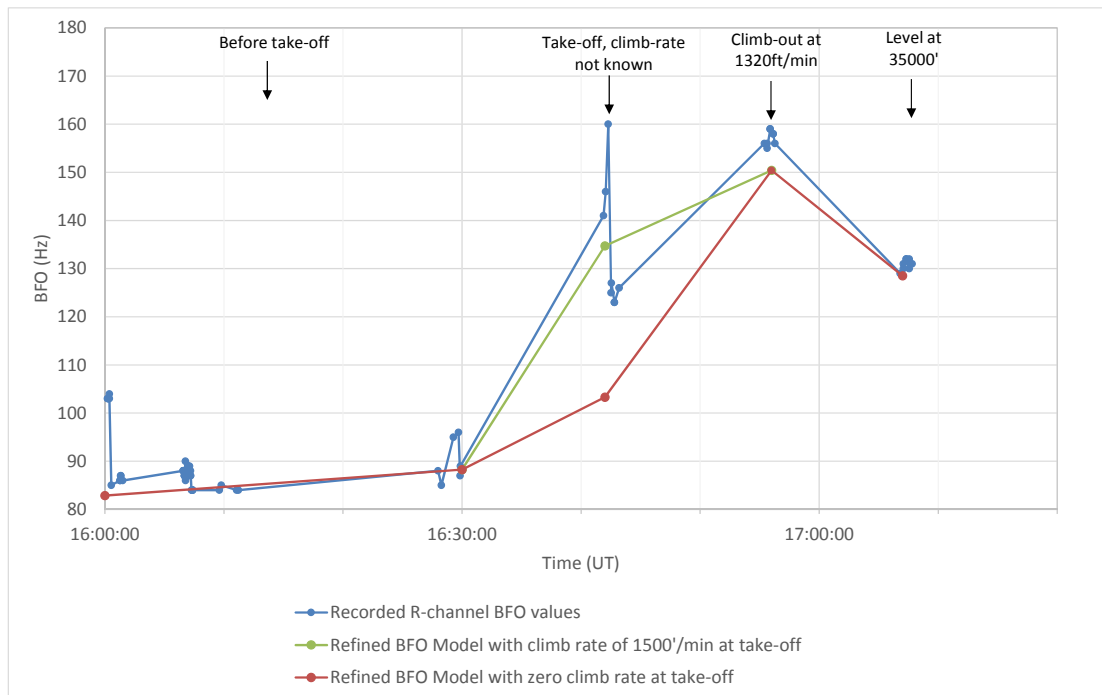


**Figure 4: BFO R-channel data and the Refined Model predictions before 17:22UT**

The aircraft is climbing between take-off at 16:42UT and 17:02UT and the uncompensated vertical speed is a strong influence on the data. The aircraft is reported level at 17:07UT so this is the only point after take-off useful for accurate comparison with the model. The model prediction is 2Hz lower than the average of the BFO values at 17:07UT, so correspondence is not perfect. However, the difference can be accounted for by a small rate of climb of 100ft/minute.

Clearly, use of data from other flights would allow a better verification (to prove or disprove the model) than is possible here.

#### *4.12 Model summary*

In summary, the Refined BFO Model described here is composed of six components.

- $D3_{\text{satellite} \rightarrow \text{ground}}$  is fully determined by the known satellite motion
- $D1_{\text{aircraft}}$ ,  $D2_{\text{aircraft}}$  and  $D2_{\text{satellite}}$  are functions of the aircraft position, speed and course and thus determined by the model.
- The constant term  $D5_{\text{offset}}$ , is determined with a small error by the BFO data before take-off.
- Only  $D4_{\text{drift}}$  is a function of time and cannot be determined from the BFO data or the model. It can be estimated from comparison with the published analysis.

The next step is to construct model tracks for the aircraft and then compare predicted BFO values for these tracks with the BFO data. If no match between the model and the data can be found for any sensible variation of the model, or only matches with a large assumed value of  $D4_{\text{drift}}$ , then the model will have failed.

If a match can be found, then this is an indication that the model corresponds to what actually happened, or at least to what the full model under the control of the investigators shows. This is discussed after the results of the track modelling below.

## 5 Radar Data

A turn-back point of 103.57E, 6.92N at 17.21UT over the South China Sea has been assumed as determined by ADS-B data [1]. The precision of this point is not a critical value for the model.

None of the reported radar data has been used as a constraint on the model. If the radar targets, particularly those over the Strait of Malacca, were correctly identified as MH370 then the reported radar positions should be consistent with a possible fit to the BFO and BTO data.

## 6 The Track Model

This section describes the input model of the track for MH370 from the 17:21UT turn-back point to the final ping-arc at 00:11UT. The stated variables are changed over their possible ranges and the predicted BFO and BTO values compared to the data.

The assumptions of the model:

1. The course can be represented by a sequence of great circle courses between the measured ping-arcs starting at the turn-back point.
2. The speed for the first leg, from 17:21 to 18:29UT is a variable in the model. The speeds used are 365kt to 555kt in 5kt steps.
3. A single speed is used for the rest of the legs from 18:29UT onwards (but different from the first leg) and is a variable in the model. The speeds used are 267 to 564kt in 2kt steps

Logic for the model:

- a. After a single great circle course, this is the simplest possible model. A single great circle course at constant speed remains a potential solution, if allowed by the data.
- b. It does not necessarily assume the aircraft maintained a single course between ping-arcs, but that the average course can be represented as a straight line, at a single speed. An exercise using a more complex interpretation of a changing course between ping-arcs did not give materially different results.
- c. The reported speed for MH370 at 17:21UT was 470kt. If the aircraft changed speed after that time to a different, steady speed, the first leg must have a different average speed to later legs, so a different average speed has to be modelled for the first leg.
- d. It is consistent with an aircraft in a speed-hold mode, though continuously turning courses may be harder to understand in terms of autopilot modes.

Consequences of the model:

- a. The heading at each ping-arc is different.
- b. There is a threshold where lower speeds are impossible because the ping-arcs are too far apart for the aircraft to travel in the time available. This is a speed of 365kt for the first leg and up to 275kt for the later part of the course.
- c. Because some of the BFO measurements are discarded for reasons explained later, the treatment of positions at 18:29 and 19.41UT is more complex and is discussed later.
- d. The first leg (17:21 to 18:29UT) as defined above does not seek to replicate possible complex tracks in that period. A more complex course is equivalent to a shorter straight line course at lower speed, as modelled.

This Track Model is similar to that used in the initial report by the Malaysian ICAO [8] with the main difference in that case all tracks after 18:29UT were forced to start a point North of Sumatra. It is not

known what Track Model was used by the Inmarsat analysis and later by others, if it was different from the model used to generate the ICAO report.

## 7 Results of using the BTO and BFO data with the Track Model

### 7.1 Use of the BTO data

The Track Model was run for a set of tracks with the speeds for the a) first and then b) subsequent legs changing as shown in Table 2.

Leg	Lowest Speed (kt)	Highest Speed (kt)	Step Size (kt)	Number of steps
First leg	365	555	5	39
Subsequent Legs	266	564	2	150

**Table 2: Speeds used in Track Model**

As has been much discussed, the ping-arc data alone allows two sets of tracks, one to the South and another to the North. The methods of discrimination between these two sets is discussed in a following section.

A collection of nearly 6000 Southern tracks (39x150) was generated (the Track model set), fitting the ends of each leg to the turn-back point and the ping-arcs determined by the BTO data. Some example tracks from the set are shown in Figure 5. A corresponding set was generated for Northern tracks.

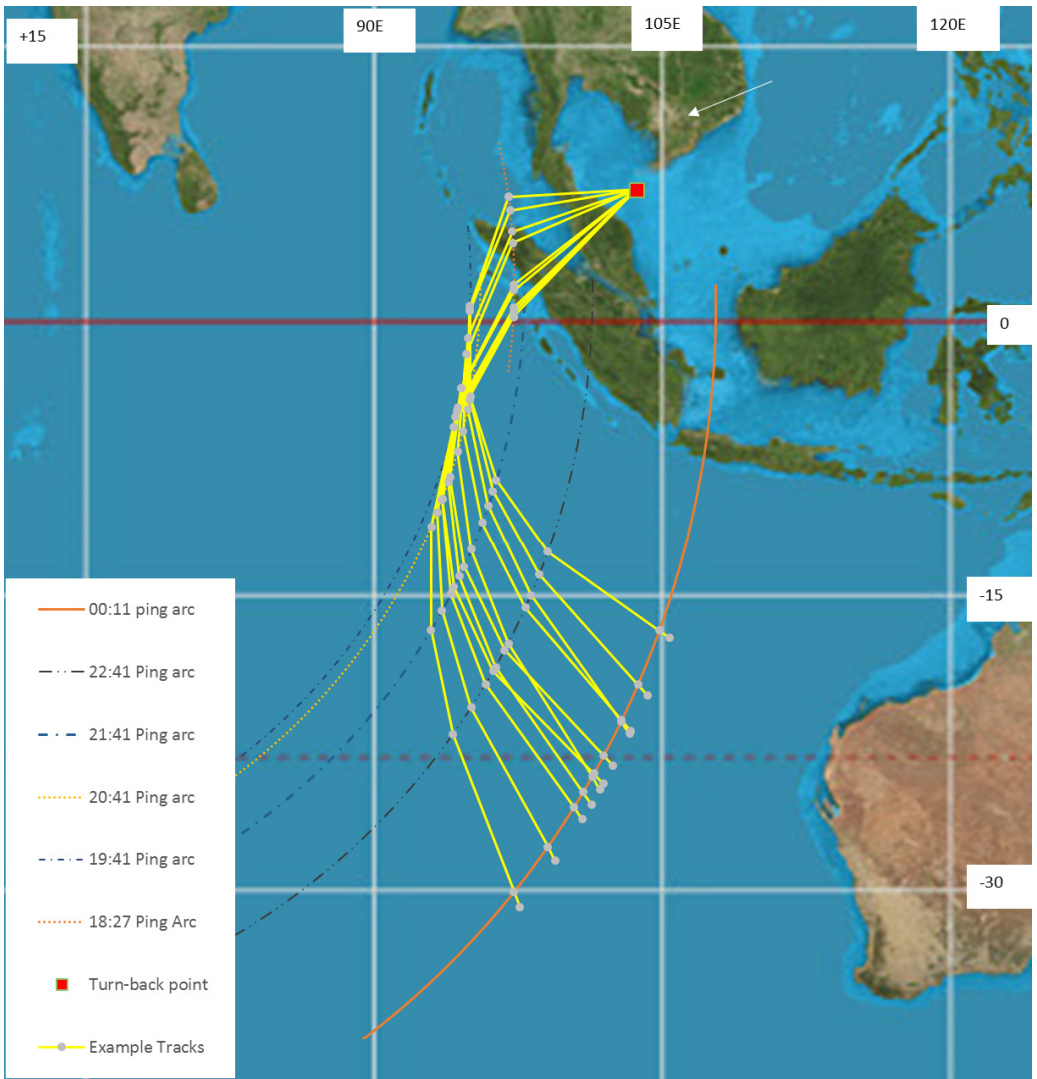


**Figure 5: Example tracks used in the track modelling. The speed for the leg to the 18:29UT ping-arc is different from the speed for the later legs in the track**

Some of the very lowest speed model tracks failed to fit to the BTO data due to the model speed being too low to allow any course that crosses both the 22:41 and 00:11UT arcs at the correct times.

## 7.2 Use of the BFO model and BFO data

The BFO model was run on the Track Model set, generating a set of BFO predictions for each of the ping-arcs where a BFO value is available. The comments in Table 3 are made on the individual BFO measurements in the data log [1].

Ping time (UT)	Issue	Consequence
18:29	Several very different values of BFO are reported in a short space of time within 3 minutes. Inmarsat state 'possible turn' in [2] but the measured BFO values could also have been caused by high rates of climb. If the data was more consistent BFO values at this time would be a very constraining on the model but the large variations mean the reported values cannot be used with any confidence.	Exclude BFO value from fit
19:41	The BFO value is a significant constraint on the fits to the Track Model. Press coverage indicates a possible concern about satellite oscillator drift in satellite eclipse. Without any calibration data that might have been obtained the measured BFO value cannot be adjusted.	Carry out the fitting process in two steps, first excluding this point and then including it.
20:41	No issue	
21:41	No issue	
22:41	No issue	
00:11	The BFO value is significantly different from models. This is discussed further below.	Exclude BFO value from fit.

**Table 3: Comments on the BFO data points and their use in the BFO Model**

a) 00:11UT BFO value – On the plot of raw BFO values, the 00:11 BFO value follows the rough linear trend of the earlier values. However, in the model the major contribution  $D_{3\text{satellite} \rightarrow \text{ground}}$  does not follow a linear trend after 22:41UT and hence the predicted BFO is not linear after that time. The predicted BFO for 00:11UT is significantly lower than the recorded data for all models. This data point is excluded from the fit and the implications of the recorded value is discussed later.

b) The inclusion or exclusion of the 19:41UT ping has a significant potential effect on the best fit tracks. This is discussed later in the paper.

Conclusion:

- For the first step in the analysis, the 20:41, 21:41 and 22:41UT BFO values are used.
- In the second step of the analysis the 19:41, 20:41, 21:41 and 22:41UT BFO values will be used.



### 7.3 North and South Tracks

The original publication of BFO data by the investigating authorities in March 2014 [2] was intended to show that all Northern tracks were excluded because none matched the BFO data. Using the set of Northern tracks discussed in section 7.1, predicted BFO values were generated using the refined BFO model. The complete set of predicted BFOs for all the Northern tracks is shown in Figure 6. Each BFO prediction is plotted separately and overlap to form the red region shown.

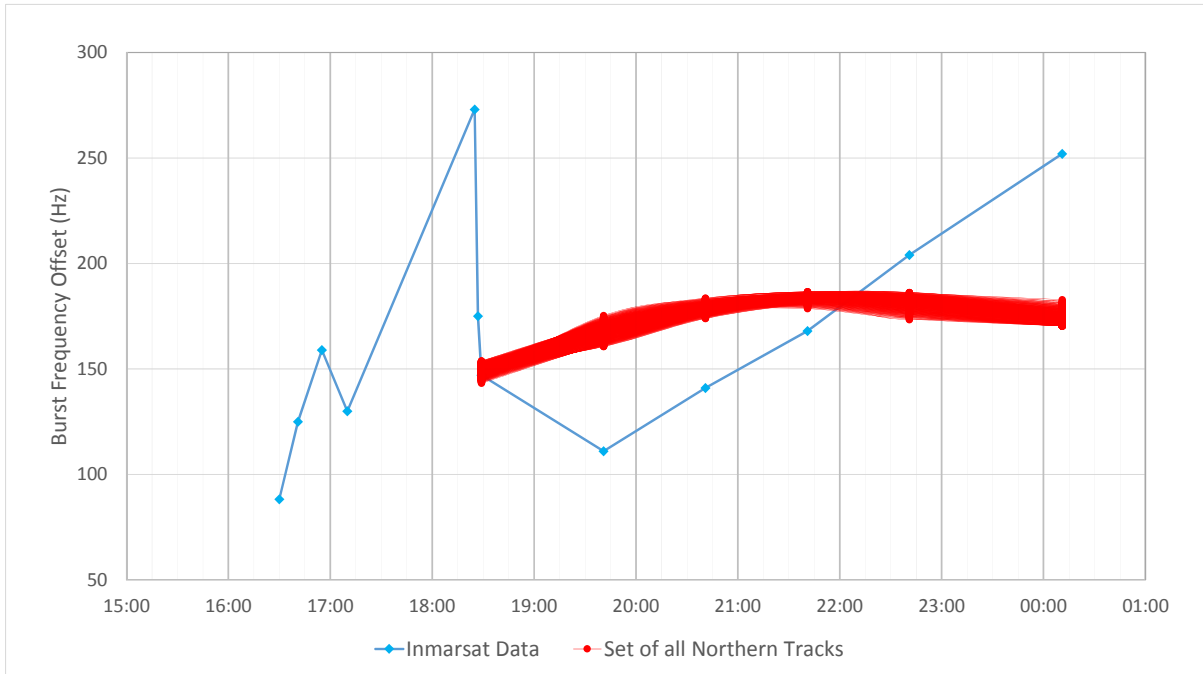


**Figure 6: Predicted BFO values for the complete set of Northern tracks**

The measured BFO data is outside the set of BFO predictions for the complete set of Northern tracks. Therefore, the track model discussed in this paper does not predict any Northern tracks that match the measured BFO data. On this basis Northern tracks are not further considered in this paper.

### 7.4 Comparisons with the Southern Tracks

The predicted BFO values for the complete set of predicted southern tracks was compared with the data on a track by track basis. As noted earlier, three BFO data points (20:41, 21:41 and 22:41UT) were used in this part of the analysis.

The differences between the data and the modelled BFOs for each track were tested using Pearson's chi-squared test [9]. The details of the statistical analysis are given in appendix E. The level of significance chosen was 90%, that is, model tracks that could not be excluded by the data with a 90% statistical confidence are regarded as possible tracks.

In the body of the paper, the results are presented a set of maps of the possible ground tracks that are compatible with the data using Pearson's chi-squared test. Details of test results are also given in appendix E.

The analysis was taken through the following steps.

### Step 1: BFO model without term $D4_{drift}$

The term  $D4_{drift}$  is the collective change of the radio-frequency oscillators in the aircraft, satellite and ground station terminals over the time period of the flight. It can only be determined by the calibration data which is not available in the public domain. Therefore, the first step is to assume this term is zero. On this basis, the map of possible final locations of the aircraft is given in Figure 7. The possible tracks are shown in pale blue and the predicted final locations at 00:19UT as purple dots. The North/South extent of the published search zones from the April ICAO report [8] is shown as red, yellow and green bars. The final search area where Ocean Shield deployed the Bluefin submarine is shown as a yellow dot, in the red search area. The interim Search area is shown to the South with a red outline. The original search areas in the Southern Ocean are not shown. The allowed aircraft speeds are those below 500kt for the first leg, and above 280kt for the later legs.

The arc of possible locations at 00:19UT overlaps the predicted search zones but also extends well to the South. The highest probability tracks do not correspond to the red-zone.

The next step is to include the term  $D4_{drift}$  and look for a better correspondence with the published search areas.

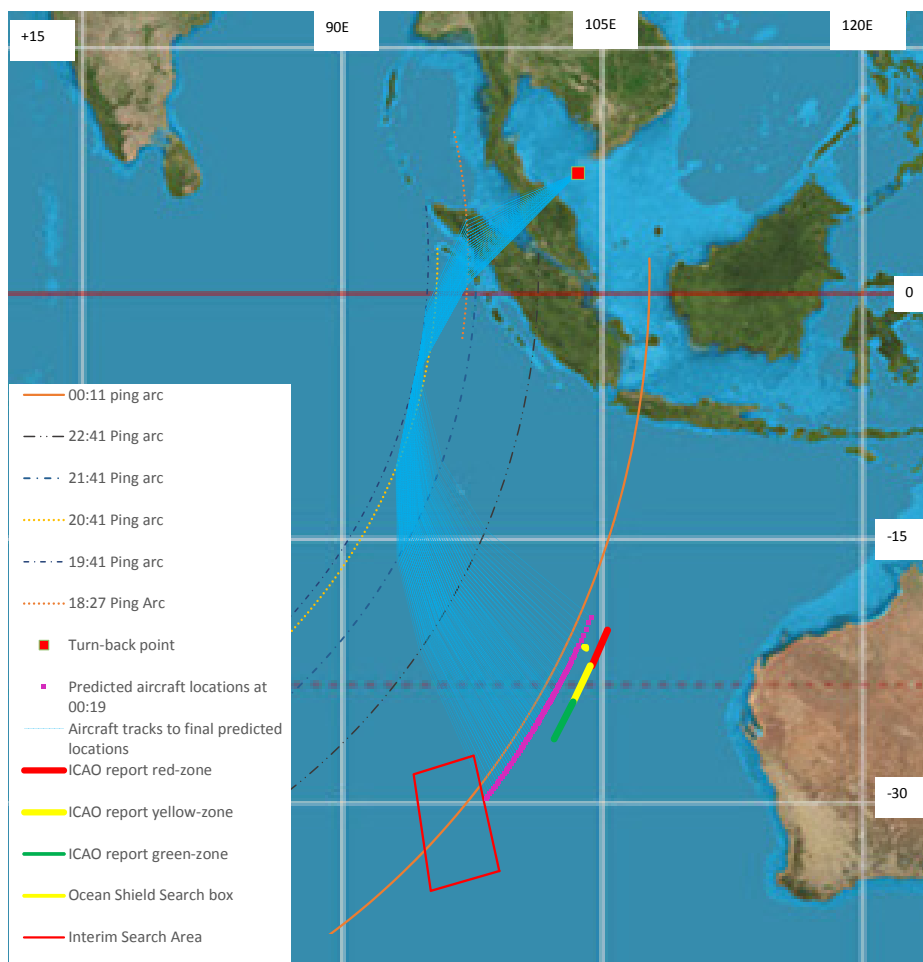


**Figure 7: Map showing tracks of the aircraft with the term  $D4_{drift}$  set to zero**

## Step 2: BFO model with term $D4_{drift}$ included

The value of  $D4_{drift}$  is unknown and cannot be computed directly without calibration data on the equipment in the transmission chain. However, the purpose of this paper is to understand what analysis was performed by Inmarsat and other parties. Therefore, a number of non-zero values of  $D4_{drift}$  were used to test if the resulting predicted tracks matched the final published search areas.

The simplest model of  $D4_{drift}$  is a linear function of time after the terminal was turned on at the airport. A model was used with value of  $D4_{drift}$  zero at a time before take-off (16:30UT) and with values between -3Hz and +3Hz at 00:11UT.

### Step 2a: BFO model with linear term $D4_{drift}$ equal to -1Hz at 00:11UT

Given this choice of the drift term, the map of possible final locations of the aircraft is shown in Figure 8.

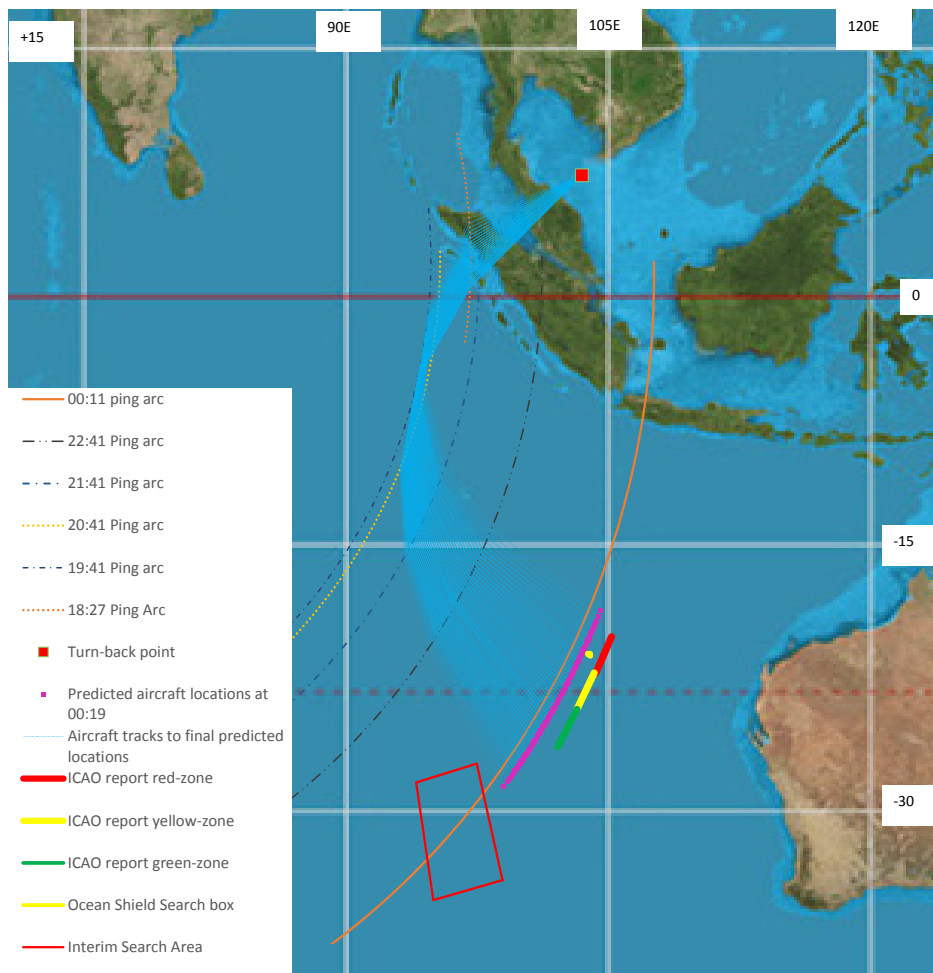


**Figure 8: Map showing tracks of the aircraft with the term  $D4_{drift}$  set to -1**

In this case the arc of best fit tracks overlaps the search areas with an extension to the South towards the Interim search area. Again, the best fit tracks do not match the red search zone.

**Step 2b: BFO model with linear term  $D4_{drift}$  equal to -2Hz at 00:11UT**

Given this choice of the drift term, the map of possible final locations of the aircraft is shown in Figure 9.

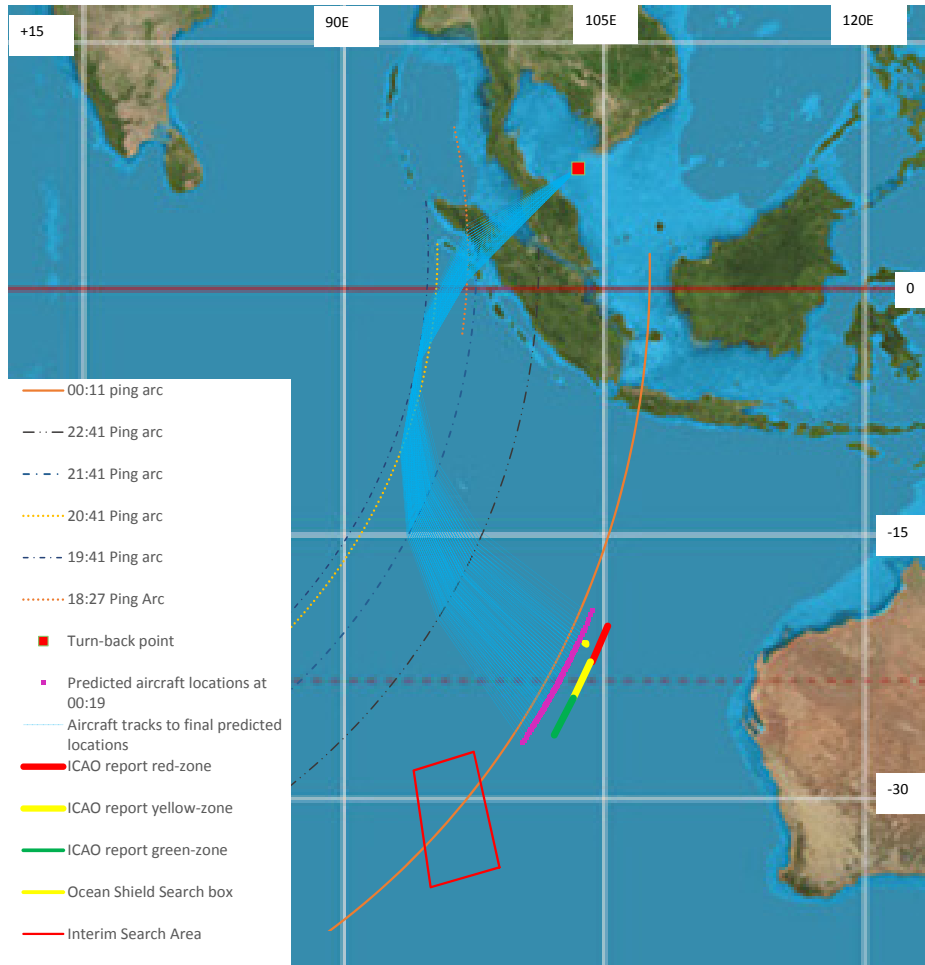


**Figure 9: Map showing tracks of the aircraft with the term  $D4_{drift}$  set to -2**

The predicted final locations of the aircraft at 00:19 are a close match to the published search areas. The highest probability tracks match the red search zone.

The plot of the BFO data and prediction for an example possible track (450kt on the 1<sup>st</sup> leg and 290kt on the later legs) is shown in Figure 10. Note here that the BFO measurements at 16:55 and 17:07UT use the climb rates from the ADS-B data (zero in the latter case). The BFO measurement at 16:42 (take-off) has been excluded from the plot as the climb rate is not recorded in the ADS-B data.

The rapidly changing BFO values at around 18:29UT mean any BFO data for that time cannot be trusted as discussed earlier. The 19:41UT data point is not used at this stage for the reasons previously stated.

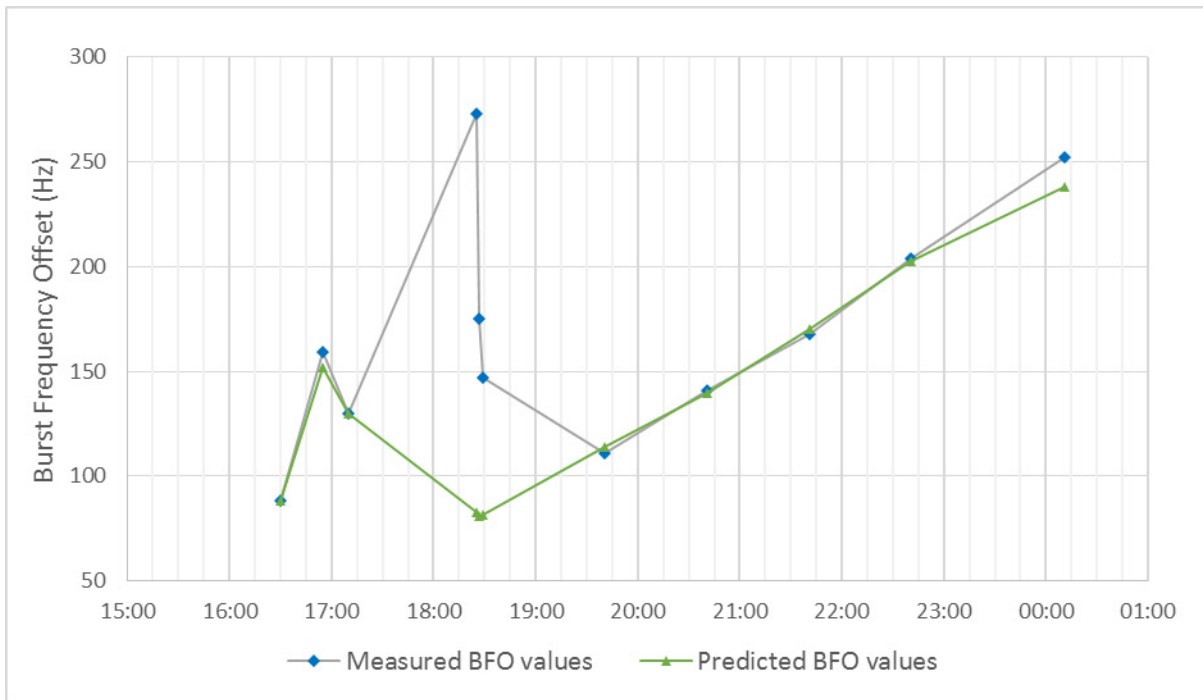


**Figure 10: BFO plot for example possible track excluding the 19:41UT data point from the BFO model fit (450kt first leg, 290kt later legs)**

The components of the refined BFO model for this case are given in appendix F.

### Step 2d: Other BFO models

A value of  $D4_{\text{drift}} = -3$  was also tried. In this case the best fit tracks do not terminate in the red search zone. Positive values of the linear drift term  $D4_{\text{drift}}$  and other simple models for the drift term were tried but did not give better correspondence to the data than the value of  $D4_{\text{drift}} = -2$  shown in Figure 9.

### Conclusion

On this basis a value of  $D4_{\text{drift}} = -2$  was selected as giving the best match to the search areas declared by the investigators. The fitting of this parameter may also have covered other small terms that are not included in the model, in addition to any oscillator drift.

Given the very limited amount of data available, the model of the BFO given in section 4 has proved to be compatible with the published search areas with only a very small allowance for frequency drifts in the satellite terminals in the link, or other errors.

## 7.5 Effects of Wind

The potential effect of wind has to be considered. The available radiosonde data at Learmonth Airport (WA, Australia) (appendix G) indicated generally calm winds at the time (less than 10kt) at all altitudes up to 30000ft. As an example a Southerly wind at 10kt was introduced into the refined BFO model. This made the fit generally poorer; the tracks and final 00:19UT points that met the chi-squared criterion are shown in

Figure 11. The tracks still cover the width of the final search areas. The conclusion was that winds at the 10kt level were not a very significant factor in the investigators' model but would have some effect.

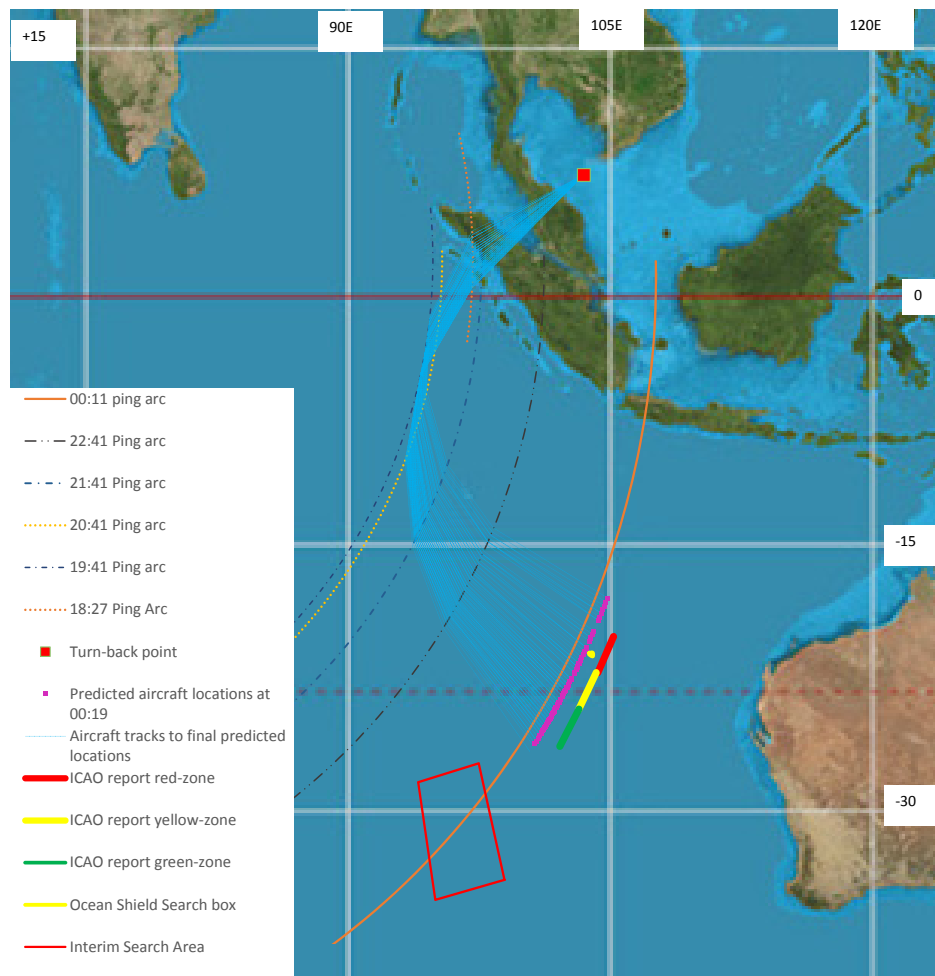


**Figure 11: Effect of the wind on the best fit tracks, Southerly wind of 10kt**

## 7.6 Further use of the Model

The Refined Model with **D4<sub>drift</sub> set to -2** can be used to look at a few ideas, particularly the possible meaning of the designated red, green and yellow search zones in the ICAO report [8].

i) Red zone – The highest probability tracks correspond to the red zone (Figure 12).

ii) Green zone – The speed at the turn-back point at 17:21UT was 470kt (from ADS-B data). The Track Model considers speeds for the first leg (17:21 to 18:29UT). The tracks for that leg with speeds between 460 and 480kt and that meet the chi-squared test are shown in Figure 13. This may indicate that the green zone corresponds to tracks with early speeds around 470kt.

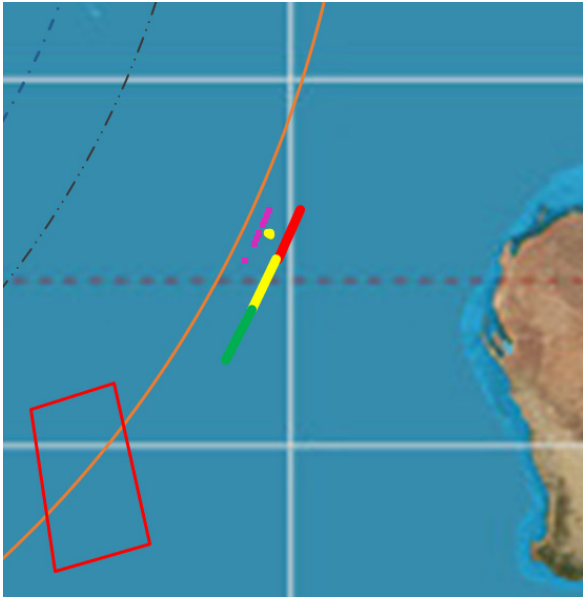


**Figure 12: Purple points show 00:19UT points for highest probability track models**

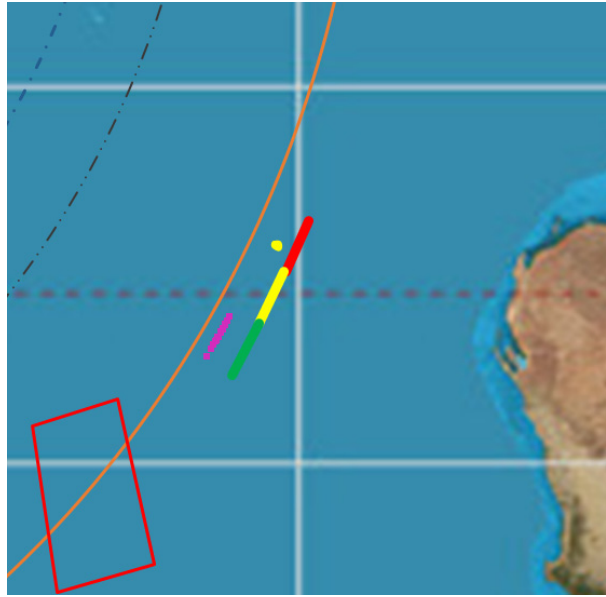


**Figure 13: Purple points show 00:19UT points for tracks with first leg speeds between 460 to 480kt**

### 7.7 Inclusion of the 19:41UT ping data

The fitting process so far has excluded the 19:41UT BFO data. The resulting fits were a reasonable match to the published search areas. While it can be a matter of judgement over whether to include an individual point or exclude it as an 'outlier', with so few data points available, exclusion of a single point could have large implications.

It is possible that the 19:41UT BFO value was adjusted by the investigators based on analysis of potential shifts in the satellite RF oscillators during the satellite eclipse that covers that time. However, that calibration data is not available so the 19:41UT BFO value cannot be adjusted here, only included or excluded.

In this next stage of the analysis the 19:41UT ping was included in the fit and the model run again (therefore the 19:41, 20:41, 21:41 and 22:41UT ping data was used). Using again the chi-squared test, the tracks that meet this statistical requirement are shown in Figure 14. The tracks that meet the test are clearly much further South. Also the best fit tracks are in the South of the arc.

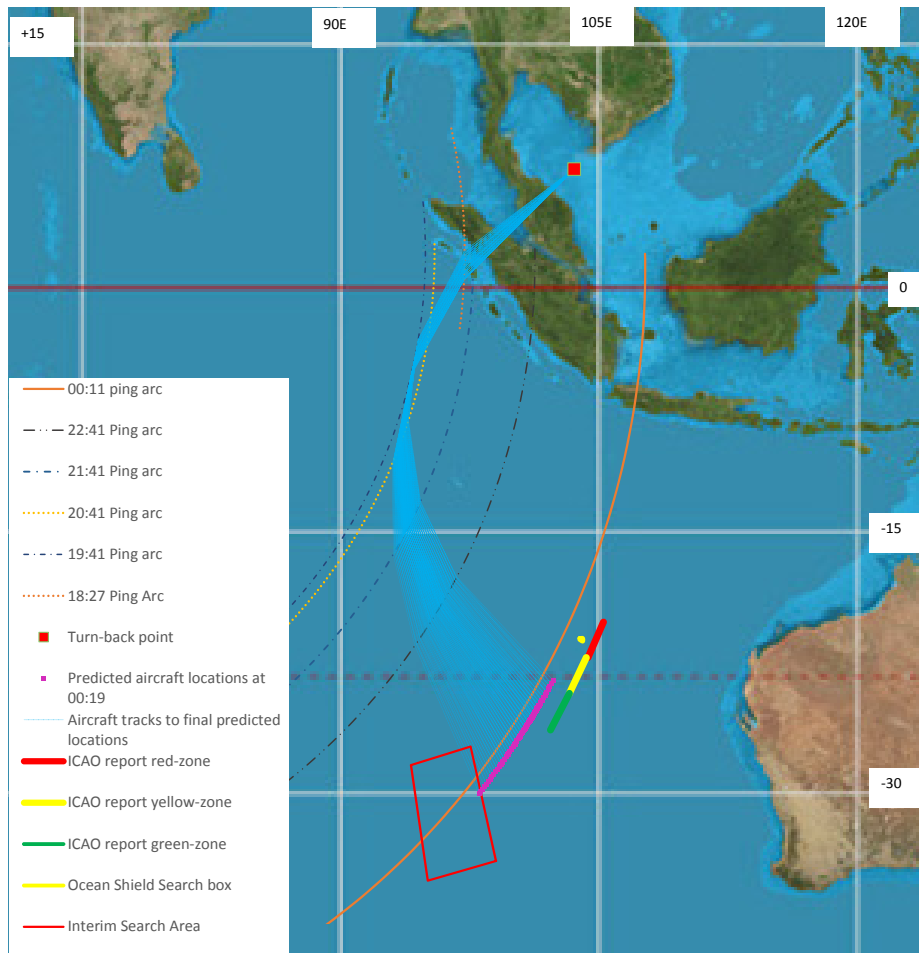


**Figure 14: Map showing tracks of the aircraft with the 19:41UT ping included in the fit**

The plot of the BFO prediction and data for an example possible track (500kt on the 1<sup>st</sup> leg and 306kt on the later legs) is shown in Figure 15. The same comments as before apply to the 18:29UT BFO values.

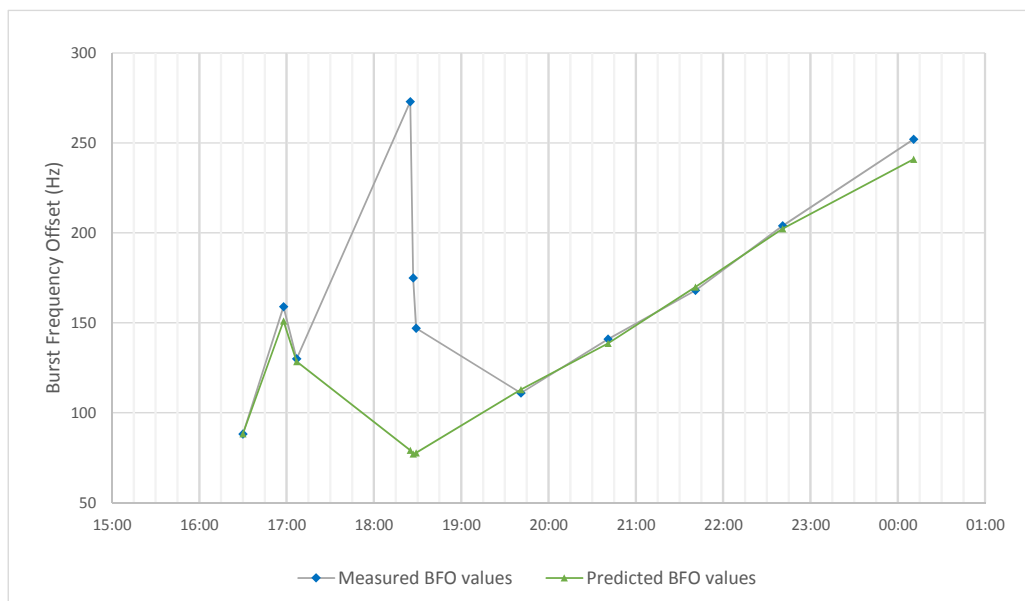


**Figure 15: BFO plot for example possible track including all the BFO data points from 19:41UT to 22:41 (500kt first leg, 306kt later legs)**



## *7.8 The 00:11UT BFO measurement and modelled value*

As stated in section 7.2 and indicated in Figure 10, the 00:11UT BFO measurement does not match to any of the best fit tracks selected using the earlier BFO measurements. The discrepancy is around 13Hz for all best fit tracks.

The model described in this paper is worked on the assumption of a constant speed course after 18:29. The Doppler shift due to climbing or descending is not corrected by the aircraft terminal and appears in the measured BFO (as during the climb after 16:42UT). On this basis the BFO discrepancy at 00:11UT can be explained by the aircraft climbing at ~900ft/min at 00:11UT.

Since at 00:11UT MH370 is taken to be within 10minutes of fuel exhaustion, this may have some impact on its expected performance in that condition. There will not be any flight experience of a B777 with a full load of passengers and freight, but virtually empty tanks, though flight simulators will have been used for investigations.

A turn to the South after 22:41UT and an increase in speed does not easily explain the discrepancy. The balance of the various components of the model means that a simple turn and increase in speed would still give a predicted value of BFO incompatible with the data at 00:11UT. Consideration of more complex courses are outside the scope of this paper.

If only the BFO data point at 00:11UT (plus all the BTO data) is used, there are predicted tracks well to the South but which require high speeds which are understood to have been ruled out on grounds of fuel usage. In any case all such tracks do **not** match the BFO data before 00:11UT so are not considered here.

## *7.9 Comparison with the Radar Data*

The consideration of the 18:29 and 19:41UT pings within the model discussed here needs to be expanded at this stage. For reasons mentioned earlier, the BFO values at these times are not used in the first phase of fitting the BFO model. Therefore the model cannot provide any verification of the geographical positions of MH370 at those times beyond the fact that the aircraft must be on the relevant ping-arc. The constant speed assumption of the model only needs to be satisfied by the time of the 20:41UT ping and later (for the fits that exclude the 19:41UT BFO value).

Thus, for example, the 18:29UT position for any of the best fit tracks can be moved North along the relevant ping arc by assuming a lower speed in the first leg (17:21 to 18:29) and a higher speed on the leg between 18:29 to 19:41. This does not affect the fit to the BFO data at 20:41 and thereafter. An example is shown in Figure 16 which shows a track that is more consistent with the radar data around 18:20UT over the Straits of Malacca.



**Figure 16: Example fitted track with 18:29UT ping position moved North by adjustment of early speeds, without affecting the BFO values at 20:41UT and later. Also shown are the best fit tracks determined earlier in the paper**

In general this paper is seeking to understand the techniques used in the Inmarsat modelling using a simple model with only one aircraft speed after 18:29UT. It does not seek to explore all the possible tracks with arbitrarily varying speeds and courses that might satisfy the BTO and BFO data.

## 8 Levels of statistical confidence

This analysis has used a 90% level of confidence in setting the threshold values in the statistical analysis. Formally this means that there is a 10% statistical chance that the correct model is excluded. A more conservative analysis would set a 99% level of confidence, i.e. a 1% chance of excluding the correct model. However, this would expand the search areas significantly. However, the data errors and confidence limits used by the investigation are not known.

## 9 Conclusions

This paper has sought to use public domain information to understand the modelling undertaken by Inmarsat, AIB and others of the satellite data from flight MH370 on March 7<sup>th</sup> and 8<sup>th</sup>, 2014. A set of simple models have been constructed working from information published by the MH370 investigation. These models are consistent with the declared search areas.

The paper has not found any major discrepancies between the released satellite data and the published conclusions. It does not attempt to alter any conclusion about the crash-site of MH370.

The Author offers his condolences to the families of the passengers and crew of MH370.

## 10 References

[1] Inmarsat raw data released 27<sup>th</sup> May 2014

<http://www.dca.gov.my/mainpage/MH370%20Data%20Communication%20Logs.pdf>

[2] Statement made by the MH370 Investigation on the Satellite data analysis 25/3/14.

[https://www.facebook.com/permalink.php?story\\_fbid=740971779281171&id=178566888854999](https://www.facebook.com/permalink.php?story_fbid=740971779281171&id=178566888854999)

[3] Description of the INMARSAT-C service for INMARSAT-3 F3 (178.1° E.L.) downloaded from FCC site

[https://www.dropbox.com/s/5y500vugqgdumpf/3F3\\_spec.pdf](https://www.dropbox.com/s/5y500vugqgdumpf/3F3_spec.pdf)

[4] System Description, Installation, and Maintenance Manual for Multi-Channel SATCOM System Types MCS-4200 and MCS-7200 <http://www.slashdocs.com/nkzyzq/sdim-msc7200-23-20-35-rev-1.html>

[5] MITEQ technical note 25T020 Enhanced Automatic Frequency Control for Inmarsat Earth Stations

<https://www.miteq.com/docs/20TEC.PDF>

[6] Paiusco, L., 'Space Mission Operations and Ground Data Systems' - SpaceOps '96, Proceedings of the Fourth International Symposium held 16-20 September 1996 in Munich, Germany. Edited by T.-D. Guyenne. ESA SP-394. Paris: European Space Agency, 1996., p.163 [http://articles.adsabs.harvard.edu/cgi-bin/nph-iarticle\\_query?1996ESASP.394..163P&defaultprint=YES&filetype=.pdf](http://articles.adsabs.harvard.edu/cgi-bin/nph-iarticle_query?1996ESASP.394..163P&defaultprint=YES&filetype=.pdf)

[7] New Data, Analysis and Luck Help Narrow Flight 370 Search Zone, Officials Factored In Satellite Temperature, Other Aircraft Speeds, Boeing Performance Calculations, April 16<sup>th</sup> 2014

<http://online.wsj.com/news/articles/SB10001424052702303887804579504142188688308>

[8] MH370 Preliminary Report and appendices by the Malaysian Ministry of Transport to the ICAO, 9<sup>th</sup> April 2014

<https://www.documentcloud.org/documents/1151155-mh370-preliminary-report.html>

<https://www.documentcloud.org/documents/1151152-mh370-actions-taken-between-0138-and-0614l.html>

<https://www.documentcloud.org/documents/1151153-mh370-cargo-manifest-and-airway-bill.html>

<https://www.documentcloud.org/documents/1151154-mh370-maps.html>

[9] [http://en.wikipedia.org/wiki/Pearson%27s\\_chi-squared\\_test](http://en.wikipedia.org/wiki/Pearson%27s_chi-squared_test)

[10] Recorded ADS-B data for MH370 on 7/3/14:

<http://uk.flightaware.com/live/flight/MAS370/history/20140307/1635Z/WMKK/ZBAA/tracklog>

Statement on the Author:

The author is a space scientist working at University College London and holds a first degree in mathematics and a doctorate in physics. He has 35 years' experience of the science and engineering of space projects and also holds a private pilot's licence. As part of his professional work he has contacts with Inmarsat but has received no payment or consideration.

The author acknowledges comments and suggestions made on a number of bulletin boards since 7<sup>th</sup> March and the suggestions of colleagues. The opinions stated are those of the author only.

## Appendix A

### List of acronyms

AAIB	Air Accident Investigation Branch
ADS-B	Automatic Dependent Surveillance-broadcast
AFC	Automatic Frequency Control
BFO	Burst Frequency Offset
BTO	Burst Timing Offset
FCC	Federal Communications Commission
GPS	Global Positioning System
Hz	Hertz
ICAO	International Civil Aviation Organisation
KIAS	Knots Indicated Airspeed
km	Kilometre
M	Metre
MTOW	maximum take-off weight
RF	Radio Frequency
TAS	True Airspeed
UT	Universal Time (GMT)

## Appendix B

### Ping Arcs distances derived from the BTO measurements

The key ping ring distances derived from the BTO data using the formulation of section 3 in the body of the paper as shown in the table.

Time (UT)	Great Circle Distance from sub-satellite point (km)
18:29	3630
19:41	3375
20:41	3436
21:41	3692
22:41	4096
00:11	4819

## Appendix C

### Determination of the term $D3_{\text{satellite} \rightarrow \text{ground}}$

The graph in Figure C-1 shows:

- the Doppler on the L-band pilot frequency from the Fucino ground station to the spacecraft
- the Doppler on the C-band pilot frequency from the spacecraft to the Perth ground station
- the sum of the two Doppler contributions, the final  $D3_{\text{satellite} \rightarrow \text{ground}}$  term

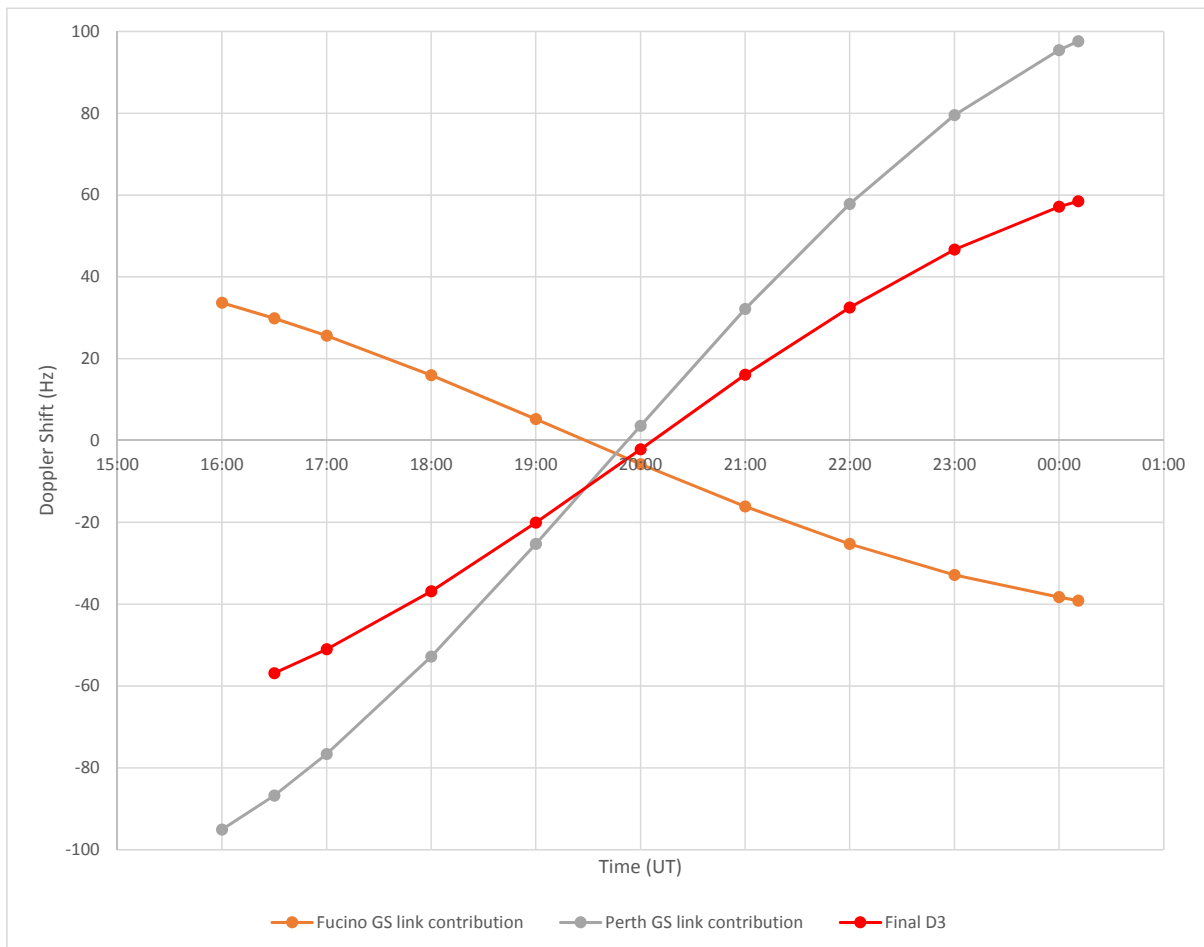
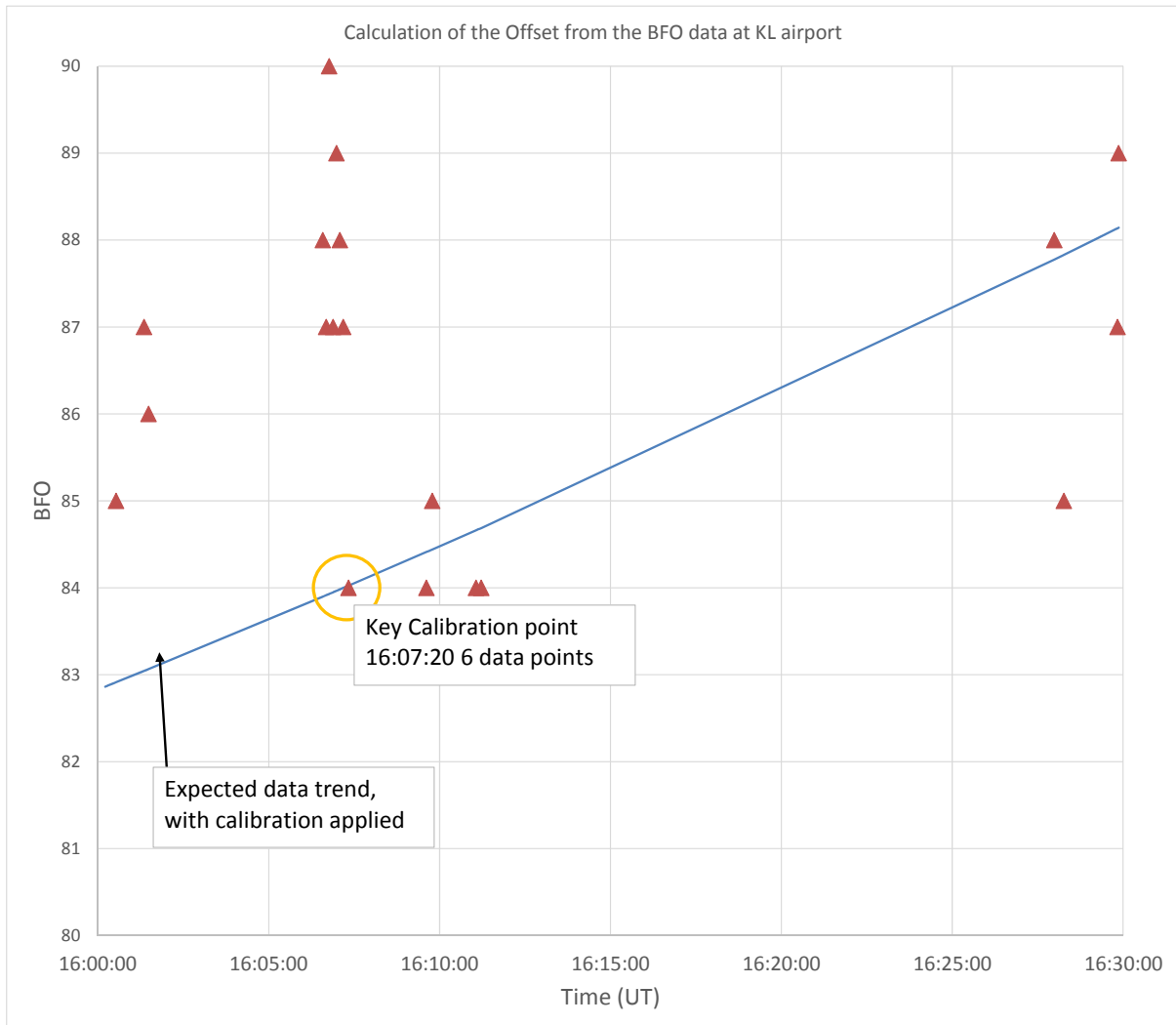


**Figure C-1: Contributions to the Term  $D3_{\text{satellite} \rightarrow \text{ground}}$**

## Appendix D

### Determination of the constant $D5_{\text{offset}}$

The graph shows the BFO values between 1600UT and 1630UT when the aircraft was at Kuala Lumpur airport. Large values of BFO are not plotted. The expected trend due to the other components of the BFO model is shown. Only R-channel values have been used, the same type as used as data in the BFO fitting. The indicated point has been used as the key calibration for setting the value of  $D5_{\text{constant}}$ .





## Appendix E

### Description of the statistical tests used for BFO data

#### A. Pearson's chi-squared test

The purpose of Pearson's chi-squared test is to exclude hypotheses that are inconsistent with a set of data after allowing for the statistical fluctuations that might have affected that data. In this case there are a small number of data points each affected by errors, so the question is which potential routes of the aircraft can be ruled out and which routes are statistically possible?

A full description of this statistical test can be found elsewhere [9] and the references therein. The chi-squared for any distribution is calculated by summing the squared differences between the data and predictions of the hypothesis, divided by the variance of the distribution (equation E-1). In this case the variance is the square of the standard deviation error of the data, earlier estimated as 2.1Hz.

$$\chi^2 = \sum_{i=1}^n \frac{(O_i - E_i)^2}{V} \quad \text{Equation E-1}$$

$\chi^2$  = Pearson's cumulative test statistic

$O_i$  = the observation

$E_i$  = the expected (theoretical) value, asserted by the hypothesis

$V$  = the variance of the distribution

$n$  = the number of data points (here this is 3 or 4).

The chi-squared statistic is compared to a value calculated from the probability that a hypothesis can be excluded, and the number of degrees of freedom (Table E-1). The number of degrees of freedom is (n-p) where n is the number of data points and p is the number of parameters being fitted, in this case the two speeds. The level of confidence chosen by the investigation for the search is not known, but 90% could be a suitable choice – that is, search in the most likely 90% of the locations of the aircraft first. However, the estimated error on the data is a key value in assessing the data and the error value of 2.1Hz used here is very much a rough estimate.

Number of data points (n)	Number of degrees of freedom (n-p, p=2)	90% confidence level	99% confidence level
3	1	2.71	6.63
4	2	4.61	9.21

**Table E-1: Chi-squared statistic for the stated confidence levels**

On this basis the chi-squared statistic is calculated using equation E-1 for the BFO data against the modelled BFO values for each track in the Track Model set. If the chi-squared statistic is greater than the values given in Table E-1 for the 90% confidence requirement, that track can be rejected.

This is a relatively simple statistical approach. Others may wish to use a different statistical method.

### **B. The fits to the data**

In the body of this paper a number of different values of the parameter  $D4_{\text{drift}}$  were used to compare the Refined BFO model to the data. In each case a matrix of chi-squared statistics was calculated from every track in the Track Model set (the set of speed choices for the first leg and then for the subsequent legs, two speeds/parameters). The speed on the first leg is shown in the top row of the matrix, the speed on the remainder of the legs in the left column. The relevant chi-squared statistic threshold from Table E-1 is applied, those matrix values that are below the threshold correspond to tracks that cannot be excluded at the 90% confidence level and are marked in green. These are the tracks and 00:19UT positions plotted on the maps in the body of this paper. The results are presented as a series of tables for each of the values of  $D4_{\text{drift}}$  used.

#### **List of tables:**

Table E-2: Fit including three BFO values between 20:41 and 22:41UT,  $D4_{\text{drift}} = 0$

Table E-3: Fit including three BFO values between 20:41 and 22:41UT,  $D4_{\text{drift}} = 0$  at 16:30, -1 at 00:11UT, linear function of time

Table E-4: Fit including three BFO values between 20:41 and 22:41UT,  $D4_{\text{drift}} = 0$  at 16:30, -2 at 00:11UT, linear function of time

Table E-5: Fit including three BFO values between 20:41 and 22:41UT,  $D4_{\text{drift}} = 0$  at 16:30, -3 at 00:11UT, linear function of time

Table E-6: Fit including three BFO values between 20:41 and 22:41UT,  $D4_{\text{drift}} = 0$  at 16:30, +1 at 00:11UT, linear function of time

Table E-7: Fit including four BFO values between 19:41 and 22:41UT,  $D4_{\text{drift}} = 0$  at 16:30, -2 at 00:11UT, linear function of time

**Table E-2: Fit including three BFO values between 20:41 and 22:41UT, D4<sub>drift</sub> = 0**

		Speed on first leg (kt)																																																	
		365	370	375	380	385	390	395	400	405	410	415	420	425	430	435	440	445	450	455	460	465	470	475	480	485	490	495	500	505	510	515	520																		
Speed on later legs (kt)	274	2.92	3.15	3.49	3.65	3.97	4.21	4.46	4.73	5.03	5.20	5.48	5.83	6.06	6.37	6.62	6.96	7.23	7.44	7.91	8.12	8.34	8.69	9.11	20.83	21.34	21.53	21.72	21.94	22.33	22.87	23.09	12.07																		
	276	2.88	3.04	3.18	3.28	3.55	3.72	3.93	4.16	4.41	4.65	4.79	5.10	5.22	5.57	5.77	6.09	6.32	6.48	6.83	7.10	7.29	7.66	7.98	8.19	8.41	8.75	8.99	9.41	9.67	9.92	10.34	10.61																		
	278	2.79	2.88	2.99	3.14	3.23	3.36	3.53	3.71	3.92	4.15	4.26	4.53	4.63	4.94	5.06	5.39	5.54	5.90	6.05	6.23	6.47	6.81	7.00	7.27	7.49	7.70	8.08	8.41	8.63	8.87	9.11	9.36																		
	280	2.75	2.77	2.83	2.94	2.98	3.09	3.21	3.37	3.54	3.74	3.82	4.04	4.29	4.41	4.67	4.82	4.95	5.23	5.42	5.57	5.95	6.11	6.28	6.46	6.71	7.07	7.28	7.48	7.78	8.00	8.23	8.46																		
	282	2.84	2.71	2.73	2.79	2.83	2.98	3.08	3.09	3.24	3.40	3.59	3.66	3.88	3.97	4.22	4.32	4.46	4.72	4.89	5.02	5.31	5.52	5.67	5.83	6.00	6.40	6.58	6.77	6.98	7.18	7.47	7.69																		
	284	2.88	2.77	2.66	2.68	2.81	2.85	2.88	2.99	2.99	3.15	3.30	3.35	3.54	3.61	3.84	3.93	4.16	4.29	4.40	4.69	4.82	4.96	5.14	5.30	5.60	5.77	5.99	6.17	6.35	6.54	6.73	6.94																		
	286	2.96	2.80	2.73	2.69	2.71	2.74	2.79	2.85	2.94	2.93	3.06	3.09	3.27	3.32	3.51	3.59	3.81	3.91	4.02	4.26	4.40	4.52	4.65	4.97	5.12	5.27	5.42	5.59	5.81	5.99	6.17	6.52																		
	288	3.13	2.93	2.81	2.66	2.66	2.66	2.68	2.72	2.79	2.77	2.87	3.02	3.03	3.21	3.25	3.31	3.51	3.59	3.68	3.91	4.01	4.14	4.26	4.52	4.66	4.83	4.97	5.13	5.28	5.44	5.82	6.00																		
	290	3.38	2.99	2.84	2.77	2.71	2.61	2.61	2.63	2.69	2.74	2.75	2.85	2.84	3.00	3.02	3.20	3.25	3.32	3.52	3.61	3.70	3.80	4.05	4.17	4.29	4.41	4.58	4.72	4.86	5.16	5.32	5.49																		
	292	3.52	3.20	2.90	2.80	2.74	2.67	2.64	2.65	2.66	2.69	2.65	2.71	2.74	2.83	2.87	2.99	3.05	3.10	3.27	3.35	3.43	3.52	3.74	3.84	3.96	4.08	4.20	4.33	4.63	4.78	4.93	5.07																		
	294	3.71	3.34	3.13	2.96	2.78	2.71	2.66	2.63	2.61	2.62	2.57	2.65	2.72	2.73	2.72	2.87	2.87	2.92	3.08	3.13	3.20	3.40	3.48	3.58	3.67	3.78	3.90	4.15	4.27	4.40	4.53	4.71																		
	296	3.89	3.49	3.26	3.05	2.94	2.83	2.76	2.63	2.59	2.60	2.66	2.60	2.63	2.65	2.71	2.73	2.74	2.87	2.92	2.96	3.02	3.19	3.26	3.34	3.43	3.52	3.75	3.86	3.98	4.10	4.22	4.34																		
	298	4.24	3.66	3.40	3.20	3.10	2.99	2.80	2.73	2.70	2.65	2.63	2.56	2.62	2.57	2.68	2.63	2.66	2.76	2.78	2.82	2.96	3.02	3.07	3.14	3.22	3.30	3.51	3.61	3.71	3.81	3.94	4.05																		
	300	4.50	4.04	3.74	3.45	3.24	3.07	2.96	2.89	2.73	2.67	2.65	2.60	2.61	2.58	2.61	2.60	2.57	2.69	2.68	2.70	2.84	2.89	2.93	2.97	3.04	3.23	3.31	3.39	3.48	3.58	3.68	3.78																		
	302	4.80	4.29	3.96	3.61	3.48	3.22	3.08	2.96	2.86	2.70	2.74	2.61	2.66	2.55	2.57	2.57	2.64	2.61	2.63	2.65	2.73	2.77	2.81	2.85	2.90	3.06	3.13	3.20	3.28	3.37	3.46	3.56																		
	304	5.23	4.52	4.16	3.83	3.63	3.46	3.19	3.05	3.02	2.87	2.78	2.74	2.67	2.66	2.61	2.54	2.62	2.60	2.56	2.67	2.69	2.67	2.70	2.74	2.90	2.93	2.99	3.06	3.11	3.18	3.26	3.35																		
	306	5.51	4.92	4.37	4.19	3.80	3.60	3.42	3.25	3.14	3.01	2.92	2.86	2.70	2.74	2.65	2.59	2.60	2.60	2.56	2.62	2.63	2.65	2.62	2.65	2.79	2.83	2.87	2.92	2.98	3.05	3.12	3.20																		
	308	5.82	5.18	4.75	4.39	4.16	3.77	3.56	3.42	3.25	3.20	3.04	2.92	2.87	2.78	2.74	2.68	2.66	2.59	2.58	2.62	2.58	2.60	2.61	2.72	2.70	2.73	2.77	2.81	2.86	2.92	2.98	3.06																		
	310	6.31	5.51	5.05	4.61	4.36	4.12	3.89	3.68	3.48	3.35	3.14	3.09	2.94	2.91	2.79	2.81	2.68	2.65	2.65	2.64	2.60	2.60	2.57	2.66	2.68	2.70	2.72	2.77	2.81	2.87	2.93																			
	312	6.69	5.96	5.46	4.99	4.57	4.35	4.11	3.84	3.62	3.48	3.35	3.23	3.03	3.02	2.85	2.86	2.82	2.68	2.72	2.70	2.63	2.59	2.66	2.66	2.64	2.65	2.67	2.70	2.73	2.74	2.78	2.93																		
	314	7.04	6.27	5.76	5.30	4.97	4.55	4.29	4.01	3.94	3.72	3.53	3.34	3.27	3.11	3.04	2.93	2.87	2.83	2.75	2.72	2.70	2.62	2.69	2.64	2.64	2.64	2.63	2.65	2.67	2.70	2.83	2.87																		
	316	7.58	6.77	6.04	5.71	5.27	4.91	4.62	4.41	4.12	3.88	3.71	3.57	3.43	3.30	3.19	3.13	2.94	2.95	2.90	2.76	2.72	2.76	2.74	2.68	2.67	2.62	2.63	2.64	2.65	2.76	2.77	2.81																		
	318	7.94	7.16	6.57	5.99	5.52	5.20	4.89	4.60	4.30	4.22	3.97	3.71	3.66	3.47	3.38	3.22	3.10	3.09	2.97	2.91	2.82	2.79	2.76	2.73	2.71	2.70	2.66	2.62	2.71	2.72	2.74	2.77																		
	320	8.38	7.50	6.88	6.29	5.93	5.58	5.25	4.94	4.65	4.40	4.14	4.02	3.80	3.69	3.50	3.41	3.25	3.18	3.11	2.98	2.92	2.93	2.85	2.76	2.73	2.71	2.70	2.69	2.76	2.76	2.76	2.74																		
	322	8.96	8.02	7.20	6.81	6.20	5.84	5.49	5.16	4.91	4.59	4.49	4.19	4.11	3.84	3.77	3.53	3.44	3.33	3.20	3.12	3.11	3.00	2.94	2.90	2.81	2.78	2.72	2.77	2.77	2.76	2.77	2.78																		
	324	9.36	8.38	7.70	7.11	6.71	6.11	5.81	5.46	5.26	4.92	4.68	4.51	4.28	4.09	3.92	3.81	3.61	3.51	3.42	3.27	3.20	3.13	3.07	2.96	2.91	2.87	2.79	2.83	2.81	2.80	2.77	2.78																		
	326	10.04	8.82	8.11	7.60	7.01	6.60	6.21	5.84	5.49	5.20	5.00	4.76	4.56	4.36	4.17	3.96	3.88	3.64	3.54	3.45	3.41	3.21	3.15	3.08	3.03	2.98	2.95	2.92	2.89	2.83	2.82	2.81																		
	328	10.46	9.39	8.64	7.92	7.47	6.89	6.48	6.09	5.93	5.57	5.21	5.08	4.75	4.63	4.40	4.20	4.03	3.91	3.74	3.57	3.52	3.43	3.35	3.17	3.10	3.05	3.05	3.01	2.98	2.95	2.92	2.88																		
	330	10.88	9.77	9.00	8.33	7.79	7.34	6.91	6.57	6.18	5.80	5.63	5.29	5.01	4.82	4.67	4.37	4.27	4.06	3.94	3.81	3.71	3.54	3.46	3.37	3.30	3.23	3.13	3.08	3.04	3.00	2.97	2.95																		
	332	11.48	10.36	9.53	8.84	8.19	7.72	7.27	6.84	6.43	6.17	5.86	5.51	5.33	5.01	4.86	4.71	4.43	4.30	4.17	4.01	3.83	3.73	3.63	3.48	3.40	3.38	3.31	3.19	3.14	3.10	3.06	3.03																		
	334	12.00	10.82	9.98	9.19	8.67	8.19	7.72	7.27	6.83	6.50	6.23	5.92	5.55	5.39	5.16	4.92	4.77	4.46	4.33	4.23	4.11	3.92	3.76	3.66	3.57	3.53	3.45	3.34	3.28	3.23	3.18	3.14																		
	336	12.65	11.42	10.36	9.73	9.01	8.50	8.02	7.55	7.19	6.89	6.47	6.16	5.89	5.61	5.43	5.21	4.95	4.80	4.58	4.39	4.26	4.14	4.02	3.91	3.73	3.64	3.56	3.48	3.41	3.35	3.30	3.25																		
	338	13.10	11.83	10.93	10.18	9.52	8.99	8.48	8.07	7.61	7.16	6.94	6.52	6.21	5.94	5.75	5.48	5.24	4.98	4.85	4.63	4.49	4.29	4.17	4.05	3.98	3.88	3.72	3.64	3.52	3.45	3.39	3.33																		
	340	13.77	12.34	11.41	10.73	9.95	9.41	8.88	8.37	7.90	7.65	7.20	6.77	6.56	6.24	5.97	5.79	5.51	5.26	5.12	4.88	4.73	4.52	4.39	4.26	4.12	4.01	3.91	3.82	3.73	3.65	3.52	3.46																		
	342	14.32	12.96	12.00	11.07	10.48	9.91	9.36	8.83	8.33	7.93	7.60	7.24	6.81	6.59	6.31	6.01	5.82	5.63	5.31	5.14	4.98	4.83	4.62	4.41	4.32	4.20	4.09	3.99	3.90	3.81	3.69	3.63																		
344	14.78	13.39	12.40	11.63	10.84	10.25	9.68	9.14	8.71	8.36	7.87	7.50	7.26	6.95	6.62	6.33	6.03	5.84	5.67	5.42	5.17	5.01	4.86	4.74	4.61	4.35	4.24	4.13	4.03	3.93	3.85	3.77																			
346	42.62	39.29	36.87	34.72	32.99	31.49	30.03	28.80	27.41	26.17	25.39	24.20	23.46	22.31	21.62	20.70	19.93	19.34	18.44	17.89	17.18	16.65	16.13	15.36	14.87	14.40	13.93	13.48	12.89	12.47	12.06	11.66																			
348	43.66	40.47	38.00	36.03	34.03	32.50	31.00	29.55	28.14	27.42	26.07	25.38	24.10	23.43	22.21	21.58	20.67	19.89	19.24	18.67	17.84	17.30	16.59	16.04	15.53	15.04	14.56	13.89	13.44	13.00	12.58	12.17																			
350	45.42	41.92	39.38	36.91	35.30	33.72	32.18	30.69	29.44	28.13	27.10	26.05	25.06	24.05	23.31	22.16	21.53	20.84	19.77	19.18	18.60	18.03	17.48	16.90	1																										

**Table E-3: Fit including three BFO values between 20:41 and 22:41UT,  $D4_{drift} = 0$  at 16:30, -1 at 00:11UT, linear function of time**

		Speed on first leg (kt)																																																	
		365	370	375	380	385	390	395	400	405	410	415	420	425	430	435	440	445	450	455	460	465	470	475	480	485	490	495	500	505	510	515	520																		
Speed on later legs (kt)	274	2.46	2.48	2.61	2.64	2.83	2.93	3.07	3.24	3.43	3.52	3.73	3.98	4.12	4.36	4.53	4.79	4.98	5.13	5.50	5.66	5.82	6.09	6.42	16.36	16.81	16.97	17.13	17.31	17.66	18.14	18.32	8.80																		
	276	2.64	2.60	2.54	2.52	2.67	2.73	2.80	2.93	3.08	3.25	3.31	3.51	3.59	3.82	3.95	4.19	4.33	4.46	4.72	4.91	5.05	5.35	5.57	5.74	5.91	6.16	6.35	6.70	6.89	7.10	7.42	7.64																		
	278	2.78	2.67	2.62	2.62	2.57	2.60	2.66	2.74	2.85	2.97	3.00	3.17	3.23	3.42	3.50	3.73	3.82	4.08	4.19	4.30	4.46	4.73	4.87	5.06	5.22	5.37	5.69	5.92	6.10	6.28	6.47	6.67																		
	280	2.94	2.76	2.67	2.61	2.52	2.53	2.55	2.61	2.68	2.78	2.78	2.93	3.07	3.12	3.30	3.37	3.45	3.66	3.77	3.86	4.13	4.24	4.36	4.49	4.66	4.94	5.09	5.24	5.46	5.63	5.80	5.98																		
	282	3.25	2.89	2.75	2.67	2.60	2.59	2.59	2.52	2.58	2.64	2.75	2.75	2.86	2.90	3.04	3.10	3.15	3.34	3.42	3.51	3.73	3.84	3.94	4.05	4.17	4.46	4.60	4.73	4.88	5.03	5.23	5.40																		
	284	3.47	3.16	2.86	2.74	2.74	2.67	2.58	2.59	2.51	2.59	2.65	2.61	2.74	2.72	2.85	2.88	3.04	3.09	3.15	3.33	3.41	3.50	3.60	3.69	3.93	3.93	4.04	4.18	4.30	4.43	4.57	4.71	4.85																	
	286	3.74	3.37	3.09	2.94	2.82	2.75	2.69	2.66	2.64	2.55	2.58	2.52	2.63	2.59	2.72	2.72	2.86	2.88	2.94	3.10	3.15	3.23	3.31	3.52	3.60	3.70	3.81	3.91	4.05	4.18	4.30	4.58																		
	288	4.05	3.63	3.37	3.07	2.92	2.83	2.75	2.69	2.65	2.56	2.55	2.63	2.56	2.66	2.61	2.63	2.73	2.75	2.76	2.92	2.96	3.00	3.07	3.26	3.34	3.43	3.51	3.61	3.71	3.82	4.09	4.21																		
	290	4.48	3.85	3.55	3.33	3.16	2.94	2.84	2.75	2.71	2.66	2.61	2.61	2.52	2.61	2.54	2.64	2.62	2.62	2.75	2.76	2.80	2.85	2.98	3.05	3.11	3.19	3.27	3.35	3.44	3.66	3.76	3.87																		
	292	4.77	4.24	3.76	3.51	3.36	3.18	3.05	2.96	2.86	2.78	2.67	2.62	2.60	2.58	2.57	2.58	2.59	2.55	2.65	2.67	2.67	2.71	2.86	2.89	2.93	2.99	3.06	3.13	3.33	3.42	3.51	3.60																		
	294	5.11	4.54	4.18	3.85	3.54	3.37	3.22	3.08	2.96	2.85	2.72	2.73	2.70	2.65	2.56	2.63	2.54	2.54	2.59	2.59	2.61	2.69	2.73	2.77	2.81	2.82	2.88	3.06	3.13	3.20	3.28	3.36																		
	296	5.43	4.82	4.44	4.08	3.87	3.60	3.43	3.21	3.07	2.98	2.96	2.82	2.74	2.71	2.65	2.63	2.55	2.60	2.60	2.55	2.56	2.64	2.66	2.66	2.69	2.73	2.88	2.90	2.96	3.02	3.08	3.15																		
	298	5.95	5.13	4.72	4.36	4.14	3.92	3.60	3.42	3.35	3.19	3.05	2.90	2.89	2.76	2.79	2.65	2.63	2.62	2.58	2.57	2.60	2.61	2.59	2.61	2.60	2.63	2.76	2.80	2.85	2.89	2.92	2.98																		
	300	6.31	5.65	5.20	4.78	4.42	4.14	3.92	3.75	3.51	3.33	3.21	3.10	3.01	2.92	2.85	2.77	2.66	2.70	2.61	2.56	2.63	2.62	2.57	2.55	2.57	2.68	2.67	2.70	2.73	2.77	2.81	2.86																		
	302	6.75	6.04	5.55	5.06	4.82	4.41	4.17	3.94	3.73	3.48	3.45	3.23	3.21	3.01	2.92	2.87	2.85	2.74	2.70	2.67	2.63	2.61	2.60	2.55	2.55	2.62	2.63	2.65	2.64	2.67	2.71	2.75																		
	304	7.33	6.39	5.87	5.38	5.09	4.80	4.39	4.14	4.04	3.81	3.61	3.46	3.34	3.22	3.11	2.95	2.96	2.87	2.75	2.78	2.74	2.62	2.60	2.59	2.66	2.61	2.61	2.62	2.60	2.62	2.64	2.67																		
	306	7.74	6.94	6.21	5.90	5.37	5.06	4.77	4.50	4.29	4.04	3.89	3.72	3.48	3.44	3.26	3.14	3.04	2.98	2.89	2.83	2.78	2.75	2.62	2.59	2.65	2.63	2.62	2.58	2.58	2.59	2.61	2.63																		
	308	8.16	7.32	6.73	6.22	5.88	5.34	5.03	4.78	4.50	4.37	4.13	3.89	3.79	3.58	3.49	3.31	3.23	3.07	3.01	2.97	2.84	2.79	2.75	2.78	2.66	2.63	2.62	2.60	2.59	2.59	2.60	2.58																		
	310	8.80	7.77	7.15	6.55	6.19	5.84	5.50	5.18	4.87	4.63	4.33	4.19	3.96	3.84	3.63	3.59	3.35	3.27	3.16	3.09	2.98	2.93	2.80	2.82	2.78	2.74	2.68	2.60	2.59	2.58	2.57	2.57																		
	312	9.31	8.36	7.70	7.06	6.51	6.15	5.80	5.44	5.11	4.86	4.67	4.44	4.14	4.06	3.79	3.73	3.63	3.39	3.35	3.27	3.12	3.00	3.00	2.94	2.82	2.78	2.74	2.71	2.68	2.62	2.56	2.63																		
	314	9.74	8.77	8.08	7.48	7.02	6.46	6.09	5.71	5.57	5.24	4.92	4.65	4.49	4.25	4.12	3.88	3.78	3.67	3.48	3.39	3.30	3.14	3.12	3.01	2.95	2.89	2.78	2.74	2.71	2.68	2.72	2.71																		
	316	10.42	9.39	8.47	8.03	7.42	6.94	6.54	6.22	5.84	5.49	5.21	5.00	4.76	4.56	4.34	4.22	3.93	3.86	3.76	3.51	3.42	3.37	3.29	3.14	3.07	2.96	2.90	2.85	2.80	2.82	2.75	2.72																		
	318	10.88	9.89	9.13	8.40	7.77	7.34	6.92	6.51	6.12	5.96	5.60	5.24	5.10	4.83	4.65	4.40	4.21	4.12	3.90	3.79	3.63	3.49	3.40	3.31	3.23	3.15	3.02	2.91	2.91	2.87	2.83	2.79																		
	320	11.43	10.32	9.54	8.77	8.31	7.85	7.40	6.98	6.57	6.23	5.85	5.68	5.33	5.17	4.85	4.71	4.45	4.29	4.16	3.94	3.82	3.75	3.60	3.42	3.33	3.24	3.17	3.09	3.09	3.03	2.92	2.83																		
	322	12.14	10.98	9.95	9.43	8.67	8.19	7.73	7.29	6.93	6.51	6.33	5.93	5.77	5.40	5.25	4.91	4.76	4.53	4.33	4.20	4.10	3.89	3.78	3.67	3.52	3.42	3.26	3.23	3.16	3.10	3.04	2.98																		
	324	12.63	11.43	10.57	9.82	9.31	8.55	8.14	7.68	7.39	6.95	6.60	6.34	6.01	5.76	5.47	5.30	4.98	4.82	4.67	4.43	4.26	4.13	4.01	3.80	3.70	3.59	3.44	3.40	3.31	3.24	3.11	3.05																		
	326	13.44	11.97	11.08	10.43	9.69	9.17	8.66	8.17	7.70	7.32	7.03	6.68	6.41	6.09	5.83	5.53	5.37	5.02	4.86	4.71	4.59	4.29	4.16	4.03	3.91	3.80	3.66	3.56	3.47	3.33	3.25	3.18																		
	328	13.95	12.65	11.73	10.83	10.27	9.54	9.01	8.50	8.26	7.78	7.32	7.10	6.67	6.48	6.14	5.88	5.59	5.41	5.17	4.90	4.77	4.62	4.47	4.18	4.06	3.93	3.86	3.75	3.65	3.55	3.46	3.33																		
	330	14.45	13.12	12.17	11.33	10.67	10.10	9.55	9.10	8.58	8.09	7.85	7.39	7.02	6.73	6.52	6.12	5.93	5.63	5.45	5.22	5.06	4.79	4.64	4.50	4.36	4.19	3.99	3.88	3.77	3.67	3.57	3.48																		
	332	15.15	13.82	12.79	11.96	11.15	10.54	9.97	9.45	8.91	8.56	8.16	7.67	7.44	7.00	6.78	6.57	6.16	5.97	5.78	5.49	5.25	5.08	4.92	4.67	4.52	4.41	4.28	4.09	3.97	3.86	3.75	3.65																		
	334	15.76	14.35	13.33	12.39	11.73	11.12	10.53	9.98	9.42	8.97	8.62	8.20	7.73	7.49	7.18	6.82	6.61	6.20	6.00	5.82	5.63	5.34	5.10	4.94	4.78	4.65	4.51	4.30	4.17	4.05	3.94	3.83																		
	336	16.53	15.06	13.78	13.03	12.13	11.51	10.90	10.31	9.85	9.46	8.94	8.50	8.17	7.76	7.52	7.21	6.85	6.63	6.34	6.03	5.84	5.65	5.47	5.29	4.98	4.82	4.67	4.53	4.39	4.26	4.14	4.02																		
	338	17.05	15.54	14.46	13.56	12.75	12.10	11.46	10.94	10.37	9.79	9.49	8.97	8.54	8.19	7.94	7.55	7.23	6.88	6.66	6.37	6.16	5.86	5.67	5.48	5.32	5.15	4.92	4.77	4.54	4.41	4.28	4.16																		
	340	17.83	16.14	15.03	14.21	13.26	12.59	11.94	11.30	10.72	10.39	9.81	9.28	8.99	8.57	8.22	7.95	7.57	7.25	7.02	6.68	6.46	6.17	5.97	5.78	5.51	5.34	5.17	5.01	4.85	4.70	4.49	4.36																		
	342	18.47	16.87	15.72	14.60	13.89	13.19	12.51	11.86	11.25	10.73	10.31	9.85	9.29	9.01	8.65	8.23	7.97	7.72	7.26	7.03	6.80	6.58	6.27	5.98	5.80	5.61	5.43	5.26	5.10	4.94	4.72	4.58																		
344	19.00	17.36	16.18	15.26	14.31	13.60	12.90	12.23	11.68	11.25	10.64	10.17	9.84	9.46	9.02	8.64	8.24	7.98	7.72	7.39	7.04	6.81	6.59	6.38	6.18	5.81	5.62	5.44	5.27	5.11	4.95	4.80																			
346	42.62	39.29	36.87	34.72	32.99	31.49	30.03	28.80	27.41	26.17	25.39	24.20	23.46	22.31	21.62	20.70	19.93	19.34	18.44	17.89	17.18	16.65	16.13	15.36	14.87	14.40	13.93	13.48	12.89	12.47	12.06	11.66																			
348	43.66	40.47	38.00	36.03	34.03	32.50	31.00	29.55	28.14	27.42	26.07	25.38	24.10	23.43	22.21	21.58	20.67	19.89	19.24	18.67	17.84	17.30	16.59	16.04	15.53	15.04	14.56	13.89	13.44	13.00	12.58	12.17																			
350	45.42	41.92	39.38	36.91	35.30	33.72	32.18	30.69	29.44	28.13	27.10	26.05	25.06	24.05	23.																																				

**Table E-4: Fit including three BFO values between 20:41 and 22:41UT,  $D4_{\text{drift}} = 0$  at 16:30, -2 at 00:11UT, linear function of time**

		Speed on first leg (kt)																																																	
		365	370	375	380	385	390	395	400	405	410	415	420	425	430	435	440	445	450	455	460	465	470	475	480	485	490	495	500	505	510	515	520																		
Speed on later legs (kt)	274	2.63	2.45	2.36	2.26	2.32	2.28	2.32	2.38	2.48	2.48	2.61	2.76	2.81	2.99	3.06	3.26	3.37	3.46	3.72	3.83	3.94	4.11	4.38	12.53	12.91	13.05	13.18	13.32	13.62	14.03	14.19	6.17																		
	276	3.03	2.80	2.54	2.39	2.42	2.37	2.30	2.34	2.38	2.47	2.46	2.56	2.59	2.72	2.76	2.92	2.99	3.06	3.25	3.35	3.45	3.67	3.80	3.91	4.03	4.20	4.34	4.61	4.76	4.91	5.13	5.30																		
	278	3.41	3.08	2.89	2.72	2.54	2.48	2.43	2.41	2.41	2.43	2.39	2.44	2.46	2.55	2.58	2.71	2.74	2.90	2.96	3.02	3.09	3.29	3.38	3.49	3.58	3.69	3.93	4.08	4.20	4.33	4.47	4.61																		
	280	3.77	3.38	3.14	2.93	2.70	2.61	2.53	2.48	2.45	2.45	2.37	2.46	2.49	2.46	2.56	2.56	2.58	2.72	2.74	2.79	2.94	3.01	3.08	3.15	3.24	3.45	3.54	3.64	3.77	3.88	4.00	4.13																		
	282	4.31	3.70	3.41	3.18	3.00	2.83	2.74	2.59	2.55	2.51	2.55	2.47	2.47	2.47	2.49	2.51	2.48	2.59	2.59	2.63	2.78	2.79	2.85	2.91	2.98	3.16	3.24	3.32	3.41	3.51	3.63	3.74																		
	284	4.70	4.19	3.70	3.42	3.31	3.13	2.90	2.83	2.67	2.68	2.64	2.51	2.57	2.47	2.49	2.47	2.56	2.53	2.52	2.61	2.64	2.67	2.69	2.72	2.88	2.94	3.00	3.07	3.15	3.23	3.32	3.40																		
	286	5.15	4.58	4.08	3.83	3.55	3.39	3.23	3.10	2.97	2.80	2.74	2.59	2.63	2.51	2.57	2.49	2.54	2.48	2.49	2.57	2.54	2.57	2.59	2.70	2.72	2.77	2.82	2.88	2.93	3.00	3.07	3.27																		
	288	5.59	4.98	4.56	4.12	3.82	3.63	3.45	3.29	3.14	2.98	2.86	2.88	2.72	2.75	2.61	2.59	2.58	2.54	2.47	2.55	2.53	2.50	2.51	2.63	2.66	2.66	2.68	2.72	2.77	2.83	2.99	3.06																		
	290	6.22	5.35	4.89	4.52	4.25	3.90	3.69	3.50	3.37	3.21	3.11	3.01	2.83	2.85	2.69	2.72	2.62	2.56	2.62	2.55	2.54	2.53	2.55	2.56	2.58	2.60	2.59	2.62	2.66	2.79	2.84	2.89																		
	292	6.65	5.92	5.25	4.86	4.60	4.32	4.09	3.91	3.70	3.51	3.32	3.16	3.10	2.96	2.91	2.81	2.76	2.64	2.66	2.63	2.54	2.53	2.60	2.57	2.53	2.53	2.55	2.57	2.65	2.69	2.73	2.77																		
	294	7.14	6.36	5.85	5.37	4.93	4.66	4.41	4.16	3.93	3.72	3.51	3.44	3.31	3.20	3.03	3.04	2.85	2.80	2.75	2.68	2.64	2.63	2.61	2.59	2.58	2.50	2.50	2.60	2.62	2.64	2.66	2.65																		
	296	7.60	6.79	6.25	5.74	5.43	5.01	4.73	4.43	4.18	3.99	3.89	3.68	3.48	3.40	3.23	3.16	3.00	2.97	2.91	2.78	2.73	2.73	2.70	2.61	2.59	2.57	2.64	2.56	2.57	2.58	2.60																			
	298	8.29	7.23	6.67	6.17	5.81	5.50	5.03	4.75	4.63	4.37	4.12	3.89	3.79	3.58	3.54	3.31	3.23	3.12	3.01	2.95	2.88	2.83	2.75	2.71	2.61	2.59	2.65	2.63	2.62	2.61	2.53	2.54																		
	300	8.76	7.89	7.29	6.74	6.23	5.84	5.51	5.25	4.91	4.63	4.40	4.24	4.04	3.89	3.72	3.58	3.38	3.35	3.17	3.06	3.06	2.99	2.86	2.77	2.73	2.76	2.67	2.64	2.62	2.60	2.59	2.58																		
	302	9.33	8.42	7.78	7.15	6.78	6.24	5.89	5.55	5.23	4.90	4.80	4.48	4.40	4.10	3.91	3.80	3.70	3.50	3.41	3.33	3.16	3.09	3.03	2.88	2.83	2.81	2.77	2.73	2.63	2.60	2.58	2.57																		
	304	10.08	8.89	8.22	7.56	7.17	6.78	6.23	5.88	5.69	5.39	5.07	4.82	4.63	4.41	4.24	4.00	3.93	3.77	3.56	3.52	3.43	3.21	3.13	3.06	3.06	2.91	2.86	2.81	2.73	2.69	2.65	2.63																		
	306	10.61	9.59	8.67	8.24	7.57	7.16	6.76	6.38	6.06	5.71	5.50	5.22	4.88	4.77	4.51	4.33	4.12	4.00	3.84	3.67	3.57	3.48	3.25	3.17	3.15	3.08	3.01	2.87	2.82	2.77	2.73	2.69																		
	308	11.14	10.09	9.34	8.68	8.23	7.54	7.12	6.78	6.39	6.17	5.85	5.50	5.34	5.02	4.87	4.58	4.44	4.19	4.07	3.95	3.73	3.62	3.53	3.48	3.25	3.17	3.10	3.03	2.96	2.90	2.84	2.73																		
	310	11.92	10.66	9.88	9.11	8.65	8.19	7.75	7.31	6.89	6.55	6.15	5.93	5.61	5.41	5.12	4.99	4.66	4.52	4.30	4.18	4.00	3.89	3.67	3.61	3.51	3.42	3.28	3.12	3.04	2.97	2.91	2.85																		
	312	12.55	11.40	10.58	9.77	9.08	8.59	8.13	7.68	7.24	6.88	6.63	6.29	5.90	5.74	5.37	5.23	5.08	4.74	4.62	4.48	4.24	4.06	3.97	3.86	3.65	3.54	3.45	3.35	3.27	3.14	2.99	2.98																		
	314	13.07	11.91	11.04	10.30	9.70	9.00	8.51	8.05	7.84	7.39	6.95	6.60	6.35	6.02	5.84	5.48	5.31	5.15	4.83	4.69	4.54	4.29	4.19	4.01	3.89	3.78	3.57	3.47	3.38	3.29	3.25	3.17																		
	316	13.89	12.64	11.52	10.98	10.21	9.61	9.10	8.68	8.20	7.73	7.35	7.07	6.72	6.45	6.13	5.94	5.56	5.41	5.24	4.90	4.74	4.62	4.48	4.23	4.10	3.92	3.81	3.69	3.59	3.53	3.35	3.27																		
	318	14.45	13.25	12.33	11.45	10.65	10.11	9.58	9.06	8.57	8.33	7.85	7.39	7.18	6.82	6.55	6.21	5.96	5.79	5.47	5.30	5.07	4.82	4.67	4.52	4.38	4.24	4.01	3.83	3.76	3.65	3.55	3.45																		
	320	15.11	13.78	12.83	11.90	11.32	10.75	10.19	9.64	9.12	8.69	8.19	7.97	7.50	7.28	6.84	6.63	6.29	6.04	5.85	5.53	5.36	5.21	4.98	4.71	4.56	4.41	4.27	4.14	4.05	3.92	3.72	3.56																		
	322	15.95	14.56	13.33	12.69	11.77	11.18	10.60	10.04	9.57	9.06	8.80	8.30	8.06	7.59	7.36	6.92	6.70	6.36	6.09	5.90	5.73	5.42	5.25	5.08	4.85	4.70	4.44	4.33	4.19	4.07	3.94	3.83																		
	324	16.53	15.10	14.08	13.17	12.54	11.62	11.11	10.52	10.15	9.61	9.15	8.81	8.39	8.07	7.66	7.43	6.98	6.77	6.56	6.22	5.96	5.77	5.58	5.28	5.11	4.95	4.72	4.60	4.45	4.31	4.08	3.96																		
	326	17.48	15.74	14.69	13.89	13.01	12.37	11.75	11.13	10.54	10.07	9.70	9.23	8.89	8.46	8.13	7.73	7.49	7.04	6.82	6.61	6.40	6.00	5.80	5.62	5.43	5.25	5.00	4.83	4.68	4.47	4.32	4.19																		
	328	18.07	16.55	15.46	14.38	13.71	12.82	12.18	11.55	11.22	10.62	10.06	9.77	9.23	8.95	8.52	8.19	7.78	7.54	7.23	6.86	6.65	6.44	6.23	5.83	5.64	5.46	5.29	5.12	4.96	4.80	4.64	4.40																		
	330	18.67	17.10	15.98	14.97	14.18	13.50	12.82	12.26	11.62	11.00	10.71	10.12	9.66	9.28	9.01	8.50	8.23	7.83	7.59	7.27	7.04	6.68	6.47	6.26	6.05	5.79	5.49	5.31	5.14	4.97	4.81	4.65																		
	332	19.46	17.92	16.69	15.71	14.76	14.00	13.31	12.68	12.03	11.59	11.08	10.48	10.18	9.61	9.33	9.06	8.53	8.27	8.02	7.62	7.30	7.06	6.84	6.49	6.27	6.08	5.88	5.61	5.43	5.25	5.08	4.91																		
	334	20.16	18.51	17.32	16.21	15.41	14.69	13.97	13.32	12.64	12.07	11.66	11.12	10.54	10.21	9.83	9.36	9.08	8.56	8.30	8.03	7.78	7.40	7.08	6.85	6.63	6.41	6.20	5.89	5.70	5.51	5.33	5.15																		
	336	21.04	19.34	17.85	16.96	15.89	15.15	14.41	13.70	13.14	12.67	12.04	11.49	11.07	10.56	10.25	9.84	9.39	9.11	8.74	8.31	8.05	7.79	7.55	7.30	6.86	6.64	6.42	6.21	6.00	5.80	5.61	5.43																		
	338	21.64	19.89	18.63	17.58	16.61	15.84	15.08	14.44	13.77	13.06	12.68	12.05	11.50	11.08	10.76	10.26	9.86	9.41	9.10	8.74	8.46	8.06	7.80	7.55	7.30	7.07	6.75	6.53	6.21	6.00	5.80	5.61																		
	340	22.53	20.57	19.28	18.33	17.20	16.41	15.63	14.87	14.18	13.77	13.06	12.42	12.04	11.53	11.10	10.75	10.27	9.87	9.55	9.11	8.83	8.46	8.20	7.93	7.54	7.30	7.06	6.83	6.61	6.39	6.10	5.90																		
	342	23.25	21.40	20.07	18.77	17.93	17.11	16.30	15.52	14.81	14.17	13.65	13.09	12.40	12.06	11.62	11.08	10.76	10.44	9.85	9.55	9.26	8.97	8.55	8.19	7.91	7.66	7.41	7.17	6.93	6.70	6.38	6.17																		
344	23.85	21.97	20.60	19.53	18.42	17.58	16.75	15.95	15.28	14.78	14.04	13.47	13.06	12.60	12.06	11.58	11.08	10.75	10.40	9.99	9.54	9.24	8.95	8.66	8.38	7.90	7.64	7.39	7.15	6.92	6.69	6.47																			
346	42.62	39.29	36.87	34.72	32.99	31.49	30.03	28.80	27.41	26.17	25.39	24.20	23.46	22.31	21.62	20.70	19.93	19.34	18.44	17.89	17.18	16.65	16.13	15.36	14.87	14.40	13.93	13.48	12.89	12.47	12.06	11.66																			
348	43.66	40.47	38.00	36.03	34.03	32.50	31.00	29.55	28.14	27.42	26.07	25.38	24.10	23.43	22.21	21.58	20.67	19.89	19.24	18.67	17.84	17.30	16.59	16.04	15.53	15.04	14.56	13.89	13.44	13.00	12.58	12.17																			
350	45.42	41.92	39.38	36.91	35.30	33.																																													

**Table E-5: Fit including three BFO values between 20:41 and 22:41UT,  $D4_{drift} = 0$  at 16:30, -3 at 00:11UT, linear function of time**

		Speed on first leg (kt)																																															
		365	370	375	380	385	390	395	400	405	410	415	420	425	430	435	440	445	450	455	460	465	470	475	480	485	490	495	500	505	510	515	520																
Speed on later legs (kt)	274	3.44	3.05	2.75	2.52	2.45	2.27	2.20	2.16	2.15	2.07	2.13	2.18	2.14	2.25	2.23	2.36	2.39	2.42	2.57	2.63	2.70	2.77	2.96	9.33	9.65	9.76	9.86	9.97	10.21	10.56	10.69	4.18																
	276	4.07	3.64	3.18	2.89	2.80	2.65	2.44	2.38	2.31	2.34	2.25	2.23	2.24	2.20	2.29	2.28	2.30	2.41	2.43	2.47	2.63	2.66	2.73	2.80	2.88	2.96	3.16	3.26	3.35	3.48	3.59																	
	278	4.67	4.14	3.79	3.47	3.15	2.99	2.84	2.71	2.60	2.52	2.40	2.35	2.33	2.30	2.29	2.32	2.30	2.35	2.36	2.36	2.35	2.48	2.52	2.54	2.58	2.63	2.80	2.86	2.94	3.02	3.10	3.19																
	280	5.23	4.64	4.25	3.87	3.52	3.32	3.14	2.99	2.85	2.76	2.59	2.62	2.54	2.44	2.46	2.38	2.34	2.41	2.36	2.36	2.39	2.41	2.43	2.45	2.46	2.59	2.62	2.67	2.71	2.78	2.84	2.91																
	282	6.00	5.15	4.70	4.32	4.04	3.71	3.52	3.29	3.16	3.01	2.98	2.82	2.71	2.67	2.58	2.55	2.45	2.47	2.39	2.38	2.46	2.38	2.39	2.40	2.42	2.50	2.52	2.56	2.58	2.62	2.65	2.71																
	284	6.57	5.85	5.17	4.75	4.52	4.23	3.87	3.70	3.45	3.39	3.26	3.04	3.04	2.85	2.77	2.69	2.72	2.60	2.54	2.52	2.50	2.48	2.42	2.39	2.48	2.48	2.46	2.48	2.50	2.53	2.56	2.58																
	286	7.19	6.41	5.71	5.36	4.93	4.66	4.41	4.17	3.94	3.68	3.52	3.29	3.27	3.05	3.05	2.88	2.86	2.72	2.68	2.68	2.57	2.54	2.52	2.52	2.48	2.47	2.47	2.48	2.44	2.46	2.48	2.60																
	288	7.78	6.95	6.38	5.81	5.36	5.07	4.79	4.53	4.27	4.03	3.81	3.76	3.51	3.48	3.25	3.18	3.06	2.97	2.81	2.83	2.75	2.62	2.59	2.63	2.61	2.52	2.48	2.47	2.47	2.47	2.47	2.52	2.53															
	290	8.59	7.47	6.87	6.35	5.98	5.49	5.18	4.89	4.66	4.39	4.24	4.04	3.77	3.72	3.47	3.44	3.25	3.14	3.13	2.96	2.91	2.85	2.75	2.71	2.67	2.64	2.54	2.52	2.51	2.55	2.54	2.54																
	292	9.17	8.23	7.37	6.84	6.49	6.09	5.76	5.48	5.17	4.88	4.61	4.34	4.23	3.98	3.88	3.66	3.57	3.37	3.30	3.22	3.05	2.98	2.99	2.89	2.76	2.71	2.67	2.64	2.62	2.60	2.58	2.56																
	294	9.82	8.83	8.16	7.53	6.96	6.59	6.23	5.88	5.54	5.22	4.94	4.79	4.56	4.39	4.14	4.07	3.80	3.70	3.53	3.40	3.32	3.19	3.12	3.05	2.99	2.81	2.76	2.78	2.74	2.70	2.67	2.58																
	296	10.41	9.39	8.71	8.03	7.63	7.05	6.67	6.29	5.93	5.63	5.46	5.17	4.86	4.73	4.45	4.33	4.08	3.97	3.86	3.64	3.54	3.46	3.37	3.19	3.12	3.05	3.04	2.86	2.81	2.76	2.72	2.68																
	298	11.27	9.97	9.25	8.60	8.12	7.70	7.10	6.71	6.55	6.18	5.82	5.50	5.33	5.03	4.92	4.60	4.47	4.25	4.08	3.97	3.79	3.69	3.54	3.45	3.26	3.18	3.16	3.09	3.03	2.96	2.79	2.74																
	300	11.84	10.77	10.02	9.34	8.67	8.17	7.74	7.37	6.96	6.56	6.23	6.01	5.71	5.50	5.22	5.02	4.74	4.63	4.37	4.20	4.11	4.00	3.77	3.62	3.52	3.48	3.29	3.21	3.13	3.06	2.99	2.93																
	302	12.55	11.43	10.64	9.87	9.38	8.71	8.25	7.80	7.37	6.95	6.78	6.37	6.21	5.82	5.53	5.37	5.19	4.90	4.75	4.62	4.33	4.21	4.09	3.86	3.75	3.64	3.54	3.44	3.26	3.17	3.09	3.02																
	304	13.45	12.03	11.20	10.39	9.89	9.40	8.71	8.24	7.98	7.60	7.16	6.81	6.56	6.23	6.00	5.67	5.53	5.31	5.02	4.90	4.75	4.43	4.30	4.17	4.09	3.86	3.75	3.64	3.49	3.39	3.30	3.22																
	306	14.10	12.88	11.77	11.23	10.40	9.89	9.38	8.89	8.47	8.00	7.74	7.36	6.92	6.74	6.39	6.14	5.83	5.66	5.43	5.15	5.00	4.85	4.52	4.38	4.28	4.15	4.03	3.80	3.69	3.58	3.48	3.38																
	308	14.75	13.49	12.59	11.77	11.22	10.38	9.86	9.41	8.91	8.61	8.20	7.74	7.53	7.09	6.89	6.48	6.29	5.95	5.77	5.56	5.25	5.09	4.93	4.81	4.48	4.35	4.21	4.08	3.96	3.84	3.73	3.52																
	310	15.69	14.18	13.25	12.32	11.75	11.18	10.63	10.08	9.55	9.10	8.61	8.31	7.90	7.62	7.23	7.03	6.60	6.41	6.08	5.89	5.65	5.48	5.18	5.04	4.88	4.73	4.52	4.27	4.13	4.00	3.88	3.76																
	312	16.43	15.07	14.09	13.11	12.28	11.66	11.09	10.55	9.99	9.53	9.22	8.77	8.28	8.05	7.58	7.37	7.16	6.72	6.53	6.33	5.99	5.74	5.58	5.41	5.10	4.94	4.79	4.63	4.49	4.29	4.04	3.95																
	314	17.04	15.69	14.63	13.76	13.02	12.17	11.57	11.02	10.73	10.17	9.62	9.17	8.85	8.42	8.19	7.71	7.49	7.27	6.83	6.62	6.42	6.07	5.90	5.65	5.47	5.30	5.00	4.84	4.68	4.53	4.42	4.28																
	316	17.99	16.53	15.22	14.57	13.64	12.92	12.29	11.76	11.19	10.60	10.11	9.78	9.31	8.98	8.54	8.30	7.82	7.59	7.37	6.92	6.70	6.51	6.30	5.96	5.78	5.53	5.35	5.17	5.00	4.87	4.60	4.45																
	318	18.66	17.25	16.16	15.14	14.17	13.52	12.87	12.24	11.65	11.34	10.74	10.19	9.90	9.44	9.09	8.66	8.33	8.09	7.68	7.45	7.15	6.78	6.57	6.37	6.16	5.97	5.64	5.39	5.23	5.06	4.90	4.74																
	320	19.42	17.87	16.76	15.65	14.97	14.28	13.61	12.95	12.30	11.79	11.17	10.89	10.30	10.02	9.46	9.20	8.76	8.42	8.17	7.76	7.53	7.29	7.00	6.63	6.42	6.21	6.01	5.82	5.64	5.46	5.16	4.93																
	322	20.39	18.79	17.36	16.58	15.51	14.81	14.11	13.43	12.85	12.24	11.90	11.31	10.99	10.41	10.11	9.56	9.29	8.83	8.49	8.24	7.99	7.59	7.35	7.12	6.82	6.61	6.25	6.06	5.86	5.67	5.48	5.30																
	324	21.07	19.42	18.23	17.15	16.41	15.33	14.71	14.01	13.55	12.91	12.34	11.91	11.39	11.01	10.49	10.20	9.62	9.35	9.08	8.64	8.29	8.04	7.79	7.40	7.17	6.94	6.64	6.43	6.22	6.01	5.69	5.50																
	326	22.15	20.15	18.93	17.99	16.96	16.21	15.46	14.73	14.02	13.46	13.00	12.42	12.01	11.46	11.06	10.57	10.25	9.69	9.41	9.14	8.85	8.34	8.08	7.83	7.59	7.35	6.97	6.74	6.52	6.24	6.03	5.83																
	328	22.83	21.08	19.82	18.57	17.78	16.74	15.97	15.22	14.82	14.10	13.44	13.06	12.42	12.06	11.54	11.14	10.61	10.31	9.93	9.47	9.17	8.89	8.62	8.12	7.86	7.61	7.37	7.13	6.90	6.67	6.45	6.12																
	330	23.51	21.72	20.42	19.25	18.33	17.53	16.73	16.06	15.30	14.56	14.20	13.49	12.93	12.46	12.13	11.51	11.17	10.67	10.36	9.95	9.66	9.20	8.92	8.65	8.38	8.02	7.62	7.38	7.14	6.91	6.68	6.46																
	332	24.40	22.65	21.23	20.10	18.99	18.09	17.29	16.55	15.78	15.25	14.65	13.92	13.56	12.86	12.52	12.19	11.53	11.21	10.89	10.37	9.98	9.68	9.39	8.94	8.66	8.38	8.12	7.77	7.52	7.28	7.04	6.80																
	334	25.20	23.31	21.94	20.68	19.74	18.89	18.05	17.30	16.49	15.81	15.32	14.67	13.98	13.57	13.12	12.53	12.19	11.57	11.24	10.88	10.57	10.09	9.69	9.40	9.11	8.81	8.53	8.12	7.86	7.60	7.35	7.11																
	336	26.19	24.25	22.55	21.53	20.29	19.42	18.56	17.72	17.08	16.50	15.77	15.10	14.62	13.98	13.62	13.11	12.56	12.21	11.77	11.22	10.90	10.58	10.26	9.95	9.38	9.09	8.80	8.52	8.25	7.98	7.72	7.47																
	338	26.86	24.88	23.44	22.23	21.11	20.21	19.33	18.58	17.80	16.97	16.50	15.76	15.09	14.60	14.22	13.60	13.13	12.57	12.18	11.74	11.40	10.89	10.57	10.25	9.92	9.61	9.22	8.93	8.50	8.23	7.96	7.70																
	340	27.86	25.64	24.16	23.09	21.78	20.86	19.96	19.07	18.28	17.78	16.94	16.20	15.73	15.12	14.62	14.18	13.60	13.13	12.72	12.18	11.83	11.39	11.05	10.72	10.21	9.90	9.59	9.29	9.00	8.71	8.34	8.07																
	342	28.66	26.58	25.06	23.57	22.61	21.66	20.73	19.82	19.00	18.24	17.63	16.97	16.15	15.74	15.23	14.57	14.18	13.79	13.07	12.71	12.34	11.99	11.46	11.03	10.66	10.34	10.02	9.71	9.40	9.10	8.68	8.39																
344	29.33	27.21	25.66	24.43	23.16	22.19	21.24	20.31	19.52	18.95	18.08	17.41	16.91	16.37	15.74	15.16	14.55	14.16	13.72	13.23	12.68	12.31	11.95	11.56	11.22	10.62	10.30	9.98	9.66	9.36	9.06	8.77																	
346	42.62	39.29	36.87	34.72	32.99	31.49	30.03	28.80	27.41	26.17	25.39	24.20	23.46	22.31	21.62	20.70	19.93	19.34	18.44	17.89	17.18	16.65	16.13	15.36	14.87	14.40	13.93	13.48	12.89	12.47	12.06	11.66																	
348	43.66	40.47	38.00	36.03	34.03	32.50	31.00	29.55	28.14	27.42	26.07	25.38	24.10	23.43	22.21	21.58	20.67	19.89	19.24	18.67	17.84	17.30	16.59	16.04	15.53	15.04	14.56	13.89	13.44	13.00	12.58	12.17																	
350	45.42	41.92	39.38	36.91	35.30	33.72	32.1																																										

Map showing tracks of the aircraft with the term  $D4_{drift}$  set to -3 (see table E-5). Highest probability tracks terminate South of the red zone.

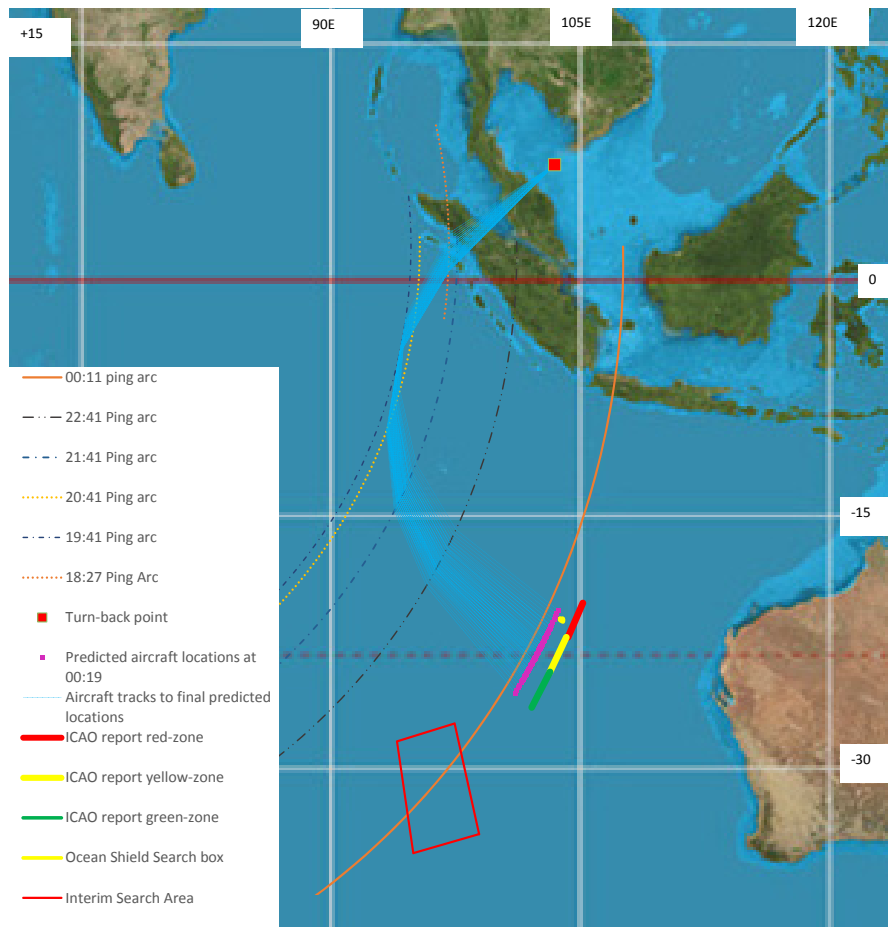


**Table E-6: Fit including three BFO values between 20:41 and 22:41UT,  $D4_{\text{drift}} = 0$  at 16:30, +1 at 00:11UT, linear function of time**

		Speed on first leg (kt)																																																	
		365	370	375	380	385	390	395	400	405	410	415	420	425	430	435	440	445	450	455	460	465	470	475	480	485	490	495	500	505	510	515	520																		
Speed on later legs (kt)	274	4.01	4.45	5.01	5.30	5.75	6.12	6.48	6.86	7.26	7.52	7.87	8.32	8.63	9.01	9.36	9.76	10.12	10.38	10.96	11.22	11.49	11.94	12.42	25.94	26.51	26.72	26.94	27.20	27.64	28.25	28.49	15.96																		
	276	3.75	4.11	4.45	4.68	5.06	5.35	5.70	6.03	6.38	6.69	6.91	7.33	7.49	7.95	8.23	8.62	8.93	9.15	9.58	9.93	10.17	10.60	11.02	11.28	11.56	11.98	12.27	12.77	13.07	13.38	13.89	14.22																		
	278	3.44	3.73	3.99	4.30	4.52	4.76	5.02	5.31	5.62	5.96	6.14	6.52	6.67	7.08	7.25	7.68	7.89	8.35	8.55	8.79	9.11	9.52	9.76	10.12	10.39	10.65	11.11	11.52	11.80	12.09	12.39	12.69																		
	280	3.19	3.42	3.63	3.89	4.07	4.28	4.51	4.76	5.04	5.33	5.50	5.78	6.14	6.34	6.67	6.91	7.09	7.44	7.71	7.91	8.40	8.61	8.83	9.06	9.40	9.83	10.10	10.36	10.74	11.01	11.29	11.58																		
	282	3.05	3.17	3.33	3.55	3.70	4.00	4.21	4.29	4.54	4.81	5.06	5.21	5.54	5.67	6.03	6.18	6.40	6.74	6.99	7.17	7.53	7.83	8.03	8.25	8.47	8.97	9.21	9.45	9.72	9.97	10.35	10.62																		
	284	2.91	3.02	3.09	3.26	3.51	3.66	3.83	4.03	4.11	4.34	4.59	4.72	4.98	5.14	5.46	5.61	5.91	6.12	6.29	6.69	6.87	7.05	7.32	7.53	7.91	8.13	8.44	8.67	8.91	9.15	9.39	9.66																		
	286	2.82	2.87	3.00	3.06	3.24	3.37	3.52	3.68	3.87	3.95	4.18	4.29	4.53	4.67	4.94	5.10	5.39	5.58	5.73	6.05	6.28	6.45	6.63	7.06	7.27	7.47	7.68	7.89	8.20	8.43	8.67	9.09																		
	288	2.86	2.85	2.89	2.87	3.02	3.13	3.25	3.39	3.56	3.62	3.83	4.04	4.14	4.38	4.51	4.63	4.93	5.06	5.24	5.54	5.70	5.92	6.09	6.42	6.61	6.87	7.07	7.28	7.49	7.70	8.19	8.43																		
	290	2.91	2.76	2.77	2.84	2.89	2.92	3.03	3.15	3.30	3.46	3.52	3.72	3.80	4.03	4.14	4.38	4.52	4.65	4.92	5.09	5.24	5.39	5.75	5.92	6.10	6.27	6.53	6.72	6.92	7.30	7.52	7.74																		
	292	2.90	2.79	2.68	2.73	2.76	2.80	2.88	2.98	3.09	3.23	3.27	3.44	3.51	3.71	3.80	4.04	4.14	4.28	4.53	4.66	4.83	4.97	5.26	5.42	5.63	5.80	5.98	6.16	6.58	6.77	6.98	7.18																		
	294	2.94	2.78	2.72	2.71	2.66	2.69	2.74	2.81	2.91	3.02	3.04	3.21	3.38	3.44	3.52	3.73	3.83	3.93	4.19	4.31	4.43	4.74	4.87	5.02	5.17	5.38	5.54	5.87	6.05	6.24	6.42	6.69																		
	296	2.98	2.79	2.71	2.66	2.65	2.69	2.73	2.68	2.75	2.86	2.99	3.01	3.16	3.22	3.39	3.47	3.56	3.77	3.87	4.00	4.11	4.36	4.49	4.66	4.80	4.95	5.25	5.47	5.64	5.81	5.98	6.17																		
	298	3.17	2.82	2.72	2.66	2.70	2.69	2.64	2.67	2.69	2.75	2.83	2.84	2.98	3.02	3.20	3.24	3.32	3.53	3.61	3.71	3.96	4.07	4.18	4.31	4.47	4.61	4.90	5.05	5.21	5.37	5.59	5.76																		
	300	3.32	3.07	2.92	2.75	2.70	2.65	2.63	2.66	2.60	2.64	2.72	2.73	2.84	2.87	3.01	3.06	3.11	3.30	3.39	3.46	3.68	3.79	3.91	4.02	4.14	4.41	4.58	4.72	4.87	5.02	5.18	5.34																		
	302	3.48	3.18	3.00	2.79	2.79	2.66	2.63	2.61	2.62	2.55	2.66	2.62	2.75	2.73	2.86	2.91	3.06	3.11	3.19	3.26	3.46	3.55	3.65	3.78	3.89	4.14	4.26	4.39	4.56	4.70	4.85	5.01																		
	304	3.75	3.29	3.08	2.91	2.82	2.74	2.62	2.58	2.63	2.57	2.59	2.65	2.65	2.74	2.75	2.77	2.92	2.96	3.01	3.20	3.28	3.35	3.44	3.54	3.77	3.90	4.01	4.13	4.25	4.38	4.52	4.66																		
	306	3.92	3.53	3.18	3.11	2.87	2.78	2.70	2.65	2.64	2.62	2.59	2.63	2.57	2.68	2.67	2.68	2.80	2.85	2.88	3.04	3.11	3.18	3.25	3.34	3.56	3.65	3.76	3.89	4.01	4.14	4.27	4.41																		
	308	4.11	3.68	3.41	3.20	3.07	2.83	2.74	2.70	2.64	2.66	2.59	2.59	2.59	2.61	2.63	2.69	2.72	2.74	2.78	2.91	2.97	3.03	3.11	3.30	3.37	3.46	3.56	3.66	3.77	3.88	4.00	4.17																		
	310	4.45	3.89	3.58	3.31	3.16	3.03	2.91	2.81	2.73	2.70	2.59	2.62	2.56	2.61	2.57	2.68	2.64	2.67	2.78	2.83	2.85	2.91	2.97	3.14	3.22	3.30	3.36	3.48	3.58	3.69	3.80	3.92																		
	312	4.72	4.20	3.86	3.55	3.28	3.18	3.05	2.87	2.77	2.73	2.66	2.65	2.54	2.62	2.54	2.63	2.64	2.60	2.72	2.76	2.78	2.81	2.96	3.01	3.08	3.15	3.23	3.32	3.41	3.49	3.62	3.85																		
	314	4.98	4.40	4.07	3.75	3.56	3.28	3.13	2.94	2.95	2.85	2.76	2.67	2.68	2.61	2.60	2.60	2.61	2.62	2.66	2.69	2.72	2.74	2.88	2.91	2.96	3.03	3.11	3.18	3.27	3.36	3.57	3.68																		
	316	5.38	4.78	4.26	4.03	3.74	3.51	3.33	3.22	3.03	2.91	2.85	2.77	2.74	2.68	2.68	2.67	2.59	2.67	2.68	2.64	2.66	2.78	2.82	2.85	2.90	2.93	2.99	3.06	3.13	3.32	3.43	3.53																		
	318	5.64	5.06	4.64	4.21	3.90	3.69	3.50	3.33	3.12	3.11	2.99	2.82	2.84	2.75	2.75	2.68	2.63	2.70	2.66	2.67	2.64	2.73	2.76	2.79	2.83	2.88	2.93	2.96	3.13	3.21	3.29	3.38																		
	320	5.97	5.31	4.85	4.43	4.19	3.95	3.74	3.54	3.37	3.21	3.07	3.01	2.90	2.85	2.78	2.75	2.68	2.70	2.69	2.65	2.66	2.75	2.73	2.74	2.78	2.81	2.86	2.91	3.07	3.13	3.22	3.28																		
	322	6.42	5.71	5.08	4.82	4.37	4.12	3.89	3.68	3.54	3.31	3.29	3.09	3.09	2.92	2.93	2.79	2.76	2.76	2.70	2.69	2.76	2.73	2.74	2.76	2.75	2.78	2.81	2.95	3.00	3.06	3.13	3.20																		
	324	6.73	5.97	5.46	5.04	4.75	4.30	4.11	3.88	3.76	3.52	3.40	3.32	3.17	3.06	3.00	2.95	2.87	2.84	2.81	2.75	2.77	2.76	2.76	2.75	2.76	2.79	2.78	2.90	2.95	3.00	3.07	3.14																		
	326	7.27	6.32	5.77	5.40	4.96	4.67	4.40	4.14	3.91	3.72	3.61	3.48	3.35	3.26	3.14	3.02	3.03	2.89	2.85	2.82	2.86	2.78	2.77	2.77	2.78	2.79	2.88	2.92	2.95	2.96	3.01	3.07																		
	328	7.60	6.76	6.18	5.64	5.31	4.88	4.59	4.32	4.23	4.00	3.74	3.69	3.46	3.43	3.29	3.16	3.10	3.05	2.95	2.87	2.90	2.88	2.86	2.79	2.79	2.79	2.89	2.91	2.94	2.97	3.02	3.08																		
	330	7.94	7.06	6.46	5.96	5.54	5.21	4.90	4.67	4.40	4.15	4.04	3.82	3.65	3.54	3.46	3.26	3.24	3.12	3.07	3.03	2.99	2.93	2.90	2.89	2.87	2.90	2.90	2.91	2.94	2.97	3.00	3.05																		
	332	8.44	7.53	6.90	6.36	5.86	5.53	5.20	4.87	4.59	4.42	4.20	3.97	3.86	3.67	3.57	3.48	3.34	3.26	3.20	3.15	3.06	3.02	2.98	2.93	2.92	2.98	2.98	2.94	2.95	2.97	3.00	3.04																		
	334	8.87	7.92	7.26	6.63	6.25	5.89	5.54	5.19	4.88	4.67	4.46	4.28	4.01	3.94	3.77	3.65	3.56	3.37	3.30	3.28	3.23	3.14	3.05	3.01	2.99	3.04	3.03	3.02	3.02	3.04	3.06	3.09																		
	336	9.41	8.41	7.56	7.06	6.52	6.13	5.77	5.43	5.16	4.96	4.64	4.45	4.25	4.08	3.97	3.84	3.68	3.59	3.45	3.38	3.32	3.26	3.21	3.17	3.12	3.09	3.08	3.07	3.07	3.07	3.09	3.11																		
	338	9.78	8.75	8.03	7.43	6.92	6.52	6.13	5.84	5.48	5.16	5.02	4.71	4.52	4.32	4.20	4.04	3.88	3.72	3.67	3.53	3.46	3.36	3.30	3.25	3.27	3.24	3.16	3.14	3.12	3.12	3.13	3.15																		
	340	10.34	9.18	8.43	7.88	7.28	6.86	6.45	6.07	5.70	5.54	5.22	4.90	4.78	4.56	4.36	4.26	4.08	3.91	3.85	3.71	3.63	3.50	3.43	3.37	3.35	3.32	3.28	3.26	3.25	3.24	3.18	3.19																		
	342	10.81	9.70	8.91	8.17	7.71	7.26	6.84	6.43	6.05	5.76	5.53	5.26	4.96	4.81	4.60	4.42	4.30	4.18	3.99	3.89	3.80	3.72	3.61	3.48	3.48	3.43	3.39	3.36	3.33	3.31	3.30	3.31																		
	344	11.20	10.06	9.25	8.63	8.00	7.54	7.10	6.68	6.37	6.10	5.74	5.47	5.32	5.08	4.85	4.66	4.46	4.34	4.26	4.08	3.93	3.84	3.76	3.74	3.67	3.53	3.48	3.45	3.42	3.40	3.38	3.38																		
	346	42.62	39.29	36.87	34.72	32.99	31.49	30.03	28.80	27.41	26.17	25.39	24.20	23.46	22.31	21.62	20.70	19.93	19.34	18.44	17.89	17.18	16.65	16.13	15.36	14.87	14.40	13.93	13.48	12.89	12.47	12.06	11.66																		
	348	43.66	40.47	38.00	36.03	34.03	32.50	31.00	29.55	28.14	27.42	26.07	25.38	24.10	23.43	22.21	21.58	20.67	19.89	19.24	18.67	17.84	17.30	16.59	16.04	15.53	15.04	14.56	13.89	13.44	13.00	12.58	12.17																		
	350	45.42	41.92	39.38	36.91	35.30	33.72	32.18	30.69	29.44	28.13	27.10	26.05	25.06	24.05	23.31	22.16	21.53	20.84	19.77	19.18	18.60	18.03	17.48	16.90	15.97	15.47	14.97	14.49	14.02	13.57	13.13	12.70																		



Map showing tracks of the aircraft with the term  $D4_{\text{drift}}$  set to +1 (see table E-6). A poor match to the search areas in indicated.

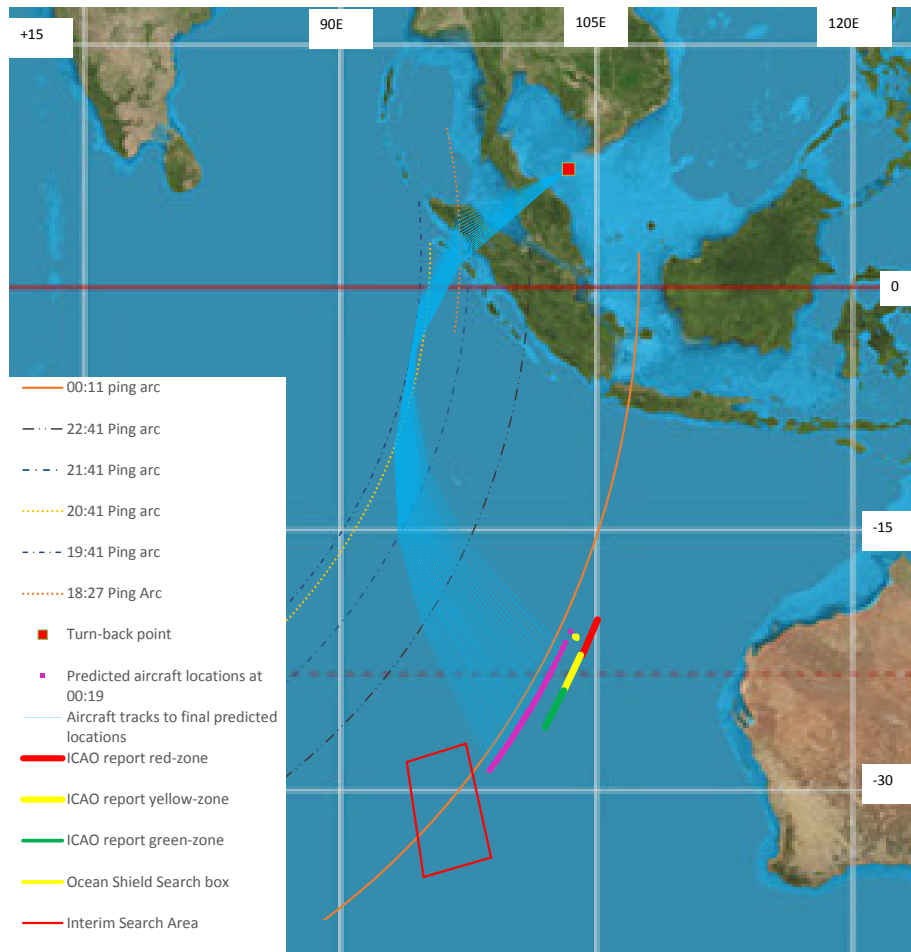


**Table E-7: Fit including four BFO values between 19:41 and 22:41UT,  $D4_{\text{drift}} = 0$  at 16:30, -2 at 00:11UT, linear function of time**

		Speed on first leg (kt)																																																	
		365	370	375	380	385	390	395	400	405	410	415	420	425	430	435	440	445	450	455	460	465	470	475	480	485	490	495	500	505	510	515	520																		
Speed on later legs (kt)	274	6.53	6.36	6.29	6.21	6.28	6.27	6.33	6.41	6.53	6.56	6.71	6.89	6.96	7.16	7.26	7.49	7.63	7.74	8.04	8.17	8.32	8.52	8.82	17.00	17.41	17.58	17.74	17.92	18.25	18.70	18.90	10.91																		
	276	6.60	6.39	6.14	6.00	6.06	6.03	5.98	6.04	6.10	6.22	6.24	6.35	6.41	6.56	6.63	6.82	6.91	7.02	7.23	7.36	7.48	7.74	7.90	8.05	8.20	8.39	8.57	8.87	9.05	9.24	9.49	9.70																		
	278	6.66	6.35	6.17	6.03	5.86	5.82	5.80	5.79	5.82	5.86	5.84	5.92	5.96	6.08	6.13	6.28	6.35	6.53	6.62	6.71	6.81	7.04	7.15	7.30	7.42	7.56	7.83	8.01	8.17	8.33	8.51	8.68																		
	280	6.72	6.35	6.12	5.92	5.72	5.65	5.59	5.56	5.55	5.58	5.52	5.63	5.69	5.69	5.81	5.83	5.88	6.05	6.10	6.18	6.35	6.45	6.55	6.65	6.77	7.01	7.13	7.27	7.43	7.57	7.73	7.88																		
	282	6.97	6.38	6.11	5.89	5.74	5.59	5.52	5.39	5.37	5.35	5.41	5.35	5.38	5.40	5.46	5.49	5.50	5.63	5.65	5.72	5.90	5.94	6.02	6.11	6.21	6.43	6.54	6.65	6.77	6.89	7.05	7.19																		
	284	7.09	6.59	6.12	5.87	5.77	5.61	5.40	5.35	5.21	5.25	5.23	5.13	5.21	5.13	5.17	5.18	5.30	5.28	5.31	5.42	5.48	5.54	5.59	5.65	5.84	5.92	6.01	6.11	6.22	6.34	6.45	6.57																		
	286	7.28	6.73	6.25	6.02	5.76	5.61	5.48	5.36	5.26	5.11	5.07	4.94	5.01	4.90	4.99	4.93	5.01	4.98	5.01	5.12	5.12	5.17	5.22	5.35	5.40	5.48	5.56	5.65	5.73	5.83	5.93	6.16																		
	288	7.48	6.88	6.48	6.07	5.78	5.61	5.45	5.31	5.18	5.04	4.94	4.99	4.85	4.91	4.79	4.79	4.80	4.78	4.74	4.85	4.85	4.84	4.89	5.03	5.08	5.11	5.16	5.23	5.31	5.40	5.59	5.69																		
	290	7.88	7.03	6.59	6.24	5.99	5.65	5.47	5.30	5.18	5.04	4.96	4.88	4.72	4.76	4.63	4.69	4.60	4.57	4.66	4.60	4.62	4.64	4.68	4.72	4.76	4.80	4.83	4.89	4.95	5.11	5.19	5.27																		
	292	8.10	7.39	6.73	6.36	6.12	5.86	5.64	5.48	5.30	5.12	4.95	4.82	4.77	4.66	4.63	4.54	4.53	4.43	4.46	4.46	4.40	4.41	4.51	4.50	4.48	4.51	4.55	4.60	4.71	4.77	4.84	4.91																		
	294	8.40	7.63	7.14	6.67	6.25	6.00	5.76	5.53	5.33	5.13	4.94	4.89	4.78	4.69	4.54	4.57	4.41	4.38	4.34	4.30	4.29	4.29	4.30	4.31	4.32	4.26	4.29	4.42	4.46	4.50	4.55	4.57																		
	296	8.67	7.87	7.36	6.86	6.57	6.16	5.90	5.62	5.39	5.21	5.13	4.93	4.76	4.70	4.55	4.50	4.36	4.34	4.31	4.20	4.18	4.20	4.19	4.12	4.12	4.13	4.23	4.17	4.20	4.23	4.27	4.31																		
	298	9.19	8.15	7.60	7.11	6.77	6.47	6.03	5.76	5.66	5.41	5.18	4.97	4.89	4.70	4.68	4.46	4.41	4.31	4.23	4.19	4.13	4.11	4.05	4.04	3.96	3.95	4.03	4.04	4.06	4.07	4.02	4.05																		
	300	9.51	8.66	8.07	7.53	7.03	6.66	6.35	6.10	5.78	5.51	5.31	5.16	4.98	4.84	4.69	4.57	4.38	4.38	4.22	4.12	4.14	4.10	3.98	3.91	3.89	3.95	3.88	3.87	3.87	3.88	3.89	3.90																		
	302	9.94	9.04	8.41	7.80	7.45	6.92	6.58	6.26	5.96	5.64	5.55	5.25	5.18	4.90	4.72	4.64	4.55	4.37	4.30	4.23	4.09	4.04	3.99	3.87	3.83	3.83	3.81	3.79	3.71	3.71	3.71	3.72																		
	304	10.56	9.39	8.73	8.09	7.71	7.33	6.80	6.45	6.28	5.99	5.68	5.45	5.28	5.07	4.91	4.69	4.63	4.50	4.31	4.28	4.21	4.00	3.94	3.89	3.90	3.78	3.75	3.72	3.66	3.64	3.62	3.62																		
	306	10.98	9.98	9.07	8.65	7.99	7.59	7.21	6.83	6.53	6.19	5.99	5.73	5.40	5.31	5.06	4.89	4.70	4.60	4.45	4.30	4.22	4.14	3.92	3.86	3.86	3.80	3.75	3.64	3.60	3.57	3.55	3.53																		
	308	11.42	10.37	9.64	8.98	8.55	7.87	7.47	7.13	6.75	6.55	6.23	5.90	5.75	5.44	5.31	5.03	4.91	4.67	4.57	4.45	4.25	4.16	4.08	4.05	3.84	3.77	3.71	3.66	3.61	3.57	3.53	3.44																		
	310	12.12	10.86	10.09	9.34	8.88	8.44	8.00	7.57	7.16	6.83	6.44	6.24	5.93	5.74	5.45	5.34	5.02	4.89	4.69	4.57	4.42	4.31	4.11	4.07	3.98	3.90	3.78	3.63	3.57	3.52	3.47	3.43																		
	312	12.68	11.53	10.72	9.92	9.24	8.76	8.30	7.86	7.43	7.08	6.84	6.51	6.13	5.98	5.62	5.49	5.35	5.02	4.92	4.79	4.55	4.38	4.31	4.21	4.01	3.92	3.84	3.76	3.69	3.58	3.44	3.45																		
	314	13.15	11.99	11.13	10.40	9.80	9.10	8.63	8.17	7.96	7.52	7.10	6.75	6.51	6.18	6.02	5.66	5.51	5.36	5.05	4.91	4.78	4.53	4.45	4.28	4.17	4.07	3.88	3.79	3.71	3.63	3.61	3.54																		
	316	13.92	12.68	11.57	11.03	10.27	9.67	9.17	8.75	8.27	7.81	7.43	7.17	6.82	6.56	6.24	6.07	5.69	5.55	5.39	5.05	4.91	4.79	4.66	4.43	4.31	4.14	4.03	3.93	3.83	3.79	3.62	3.55																		
	318	14.46	13.26	12.35	11.47	10.68	10.14	9.61	9.09	8.60	8.37	7.90	7.44	7.24	6.88	6.62	6.28	6.03	5.87	5.57	5.40	5.18	4.93	4.79	4.65	4.52	4.39	4.17	4.00	3.93	3.83	3.74	3.65																		
	320	15.11	13.78	12.83	11.90	11.32	10.76	10.20	9.66	9.13	8.71	8.21	7.99	7.52	7.31	6.87	6.67	6.33	6.08	5.90	5.59	5.42	5.27	5.05	4.78	4.64	4.50	4.37	4.25	4.16	4.05	3.86	3.70																		
	322	15.95	14.57	13.34	12.69	11.77	11.18	10.60	10.04	9.57	9.06	8.80	8.31	8.07	7.59	7.37	6.93	6.72	6.38	6.12	5.93	5.76	5.45	5.29	5.12	4.90	4.75	4.50	4.39	4.26	4.14	4.03	3.92																		
	324	16.55	15.12	14.10	13.18	12.55	11.63	11.11	10.53	10.15	9.62	9.15	8.81	8.39	8.07	7.66	7.43	6.99	6.77	6.56	6.22	5.97	5.78	5.60	5.30	5.13	4.97	4.75	4.63	4.48	4.35	4.13	4.01																		
	326	17.53	15.79	14.73	13.93	13.04	12.40	11.77	11.15	10.56	10.09	9.71	9.24	8.90	8.46	8.14	7.73	7.50	7.04	6.82	6.61	6.40	6.00	5.81	5.62	5.44	5.26	5.00	4.84	4.69	4.48	4.34	4.21																		
	328	18.17	16.64	15.54	14.46	13.78	12.88	12.23	11.60	11.27	10.66	10.10	9.80	9.26	8.97	8.54	8.21	7.80	7.56	7.24	6.87	6.65	6.44	6.23	5.83	5.64	5.46	5.29	5.12	4.96	4.80	4.64	4.41																		
	330	18.82	17.25	16.11	15.10	14.30	13.60	12.93	12.35	11.71	11.08	10.78	10.19	9.72	9.33	9.06	8.54	8.27	7.86	7.62	7.29	7.06	6.70	6.48	6.27	6.06	5.80	5.50	5.31	5.14	4.97	4.81	4.65																		
	332	19.69	18.14	16.90	15.90	14.94	14.17	13.47	12.83	12.17	11.72	11.21	10.59	10.29	9.71	9.42	9.14	8.60	8.34	8.08	7.67	7.35	7.11	6.87	6.52	6.30	6.10	5.90	5.63	5.44	5.26	5.08	4.92																		
	334	20.48	18.81	17.60	16.48	15.67	14.93	14.20	13.54	12.84	12.27	11.84	11.29	10.70	10.37	9.97	9.49	9.20	8.68	8.41	8.13	7.87	7.48	7.16	6.92	6.69	6.47	6.25	5.93	5.73	5.54	5.36	5.18																		
	336	21.46	19.73	18.23	17.32	16.24	15.47	14.73	14.00	13.43	12.94	12.30	11.73	11.31	10.78	10.46	10.04	9.57	9.28	8.90	8.46	8.19	7.93	7.67	7.42	6.97	6.73	6.51	6.29	6.08	5.87	5.67	5.48																		
	338	22.18	20.40	19.12	18.04	17.06	16.27	15.49	14.83	14.14	13.42	13.02	12.38	11.81	11.38	11.05	10.53	10.12	9.65	9.34	8.96	8.67	8.25	7.99	7.72	7.47	7.22	6.90	6.66	6.33	6.11	5.91	5.70																		
	340	23.19	21.20	19.89	18.92	17.77	16.95	16.15	15.37	14.66	14.23	13.51	12.85	12.45	11.92	11.48	11.11	10.62	10.20	9.87	9.41	9.11	8.74	8.45	8.17	7.77	7.52	7.27	7.02	6.79	6.56	6.26	6.04																		
	342	24.05	22.18	20.81	19.49	18.62	17.78	16.95	16.14	15.41	14.75	14.21	13.63	12.92	12.56	12.10	11.54	11.20	10.86	10.26	9.94	9.63	9.32	8.89	8.51	8.22	7.95	7.69	7.43	7.18	6.94	6.60	6.38																		
344	24.81	22.89	21.50	20.39	19.25	18.38	17.53	16.71	16.01	15.49	14.72	14.13	13.70	13.21	12.66	12.16	11.63	11.28	10.92	10.49	10.01	9.70	9.39	9.07	8.78	8.28	8.01	7.74	7.48	7.23	6.99	6.75																			
346	42.62	39.29	36.87	34.72	32.99	31.49	30.03	28.80	27.41	26.17	25.39	24.20	23.46	22.31	21.62	20.70	19.93	19.34	18.44	17.89	17.18	16.65	16.13	15.36	14.87	14.40	13.93	13.48	12.89	12.47	12.06	11.66																			
348	43.66	40.47	38.00	36.03	34.03	32.50	31.00	29.55	28.14	27.42	26.07	25.38	24.10	23.43	22.21	21.58	20.67	19.89	19.24	18.67	17.84	17.30	16.59	16.04	15.53	15.04	14.56	13.89	13.44	13.00	12.58	12.17																			
350	45.42	41.92	39.38	36.91	35.30	33.72	32.18	30.69	29.44	28.13	27.10	26.05	25.06	24.05	23.31	22.16	21.53	20.84	19.77																																

## Appendix F

### Plots of the components of the Refined BFO Model

The graphs below show the elements of the Refined BFO model for examples track in the Track Model set, broken down as described in this paper, and also the final fits to the BFO data.

$$BFO = D1_{aircraft} + D2_{aircraft} + D2_{satellite} + D3_{satellite \rightarrow ground} + D4_{drift} + D5_{offset}$$

#### A. Three data point fit

Components of an example fit to the 20:41, 21:41 and 22:41UT BFO points are shown in figure F-1. The two components  $D1_{aircraft} + D2_{aircraft}$  (Doppler due to aircraft speed and the pre-applied compensation in aircraft satellite terminal) are added together before they are plotted as they are individually very large and would make the plot of the rest of the components hard to read. Component  $D4_{drift} = -2$  at 00:11UT – the best fit to the published search areas.

In this graph the 19:41UT BFO value is plotted with zero climb rate component.

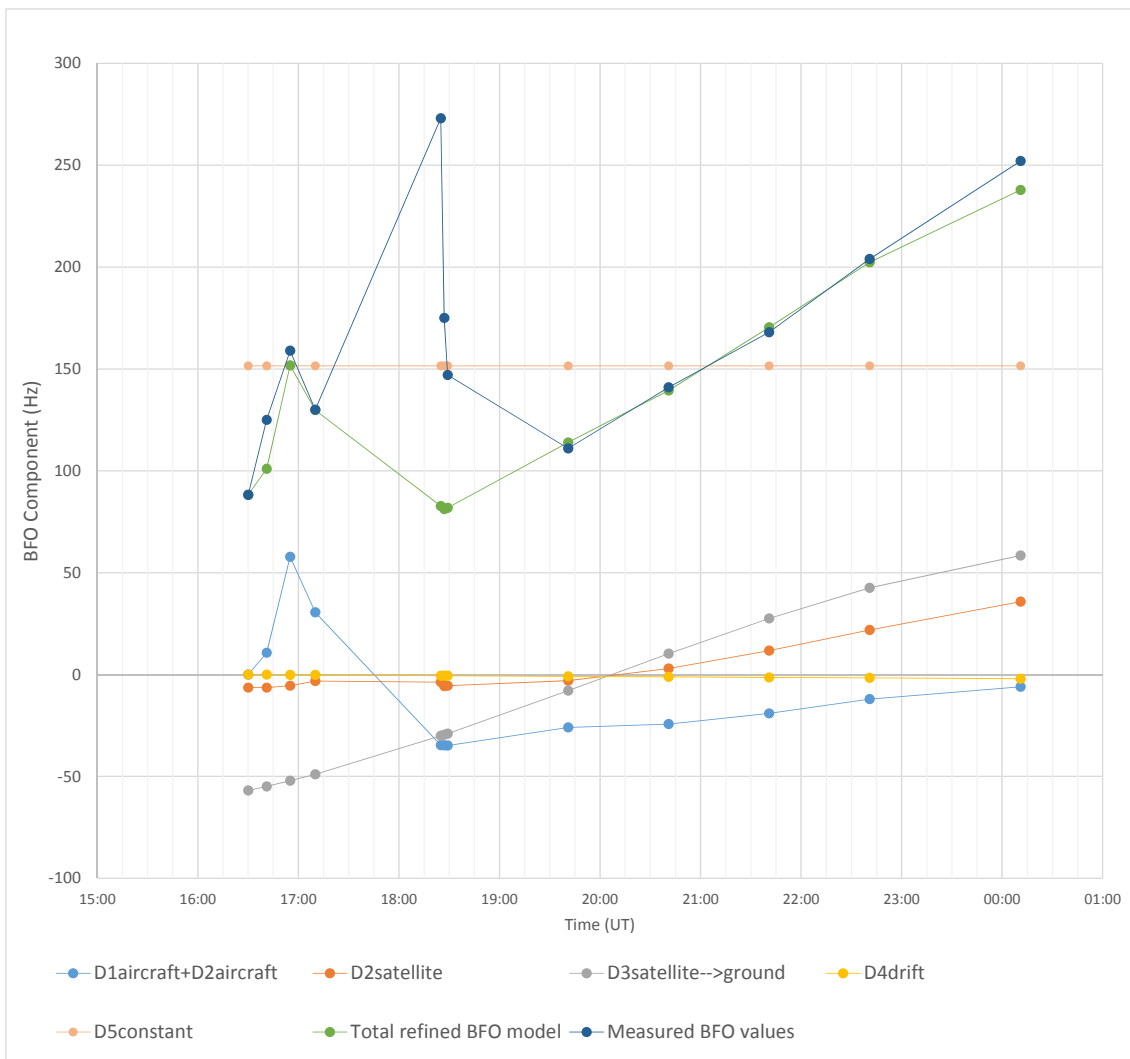
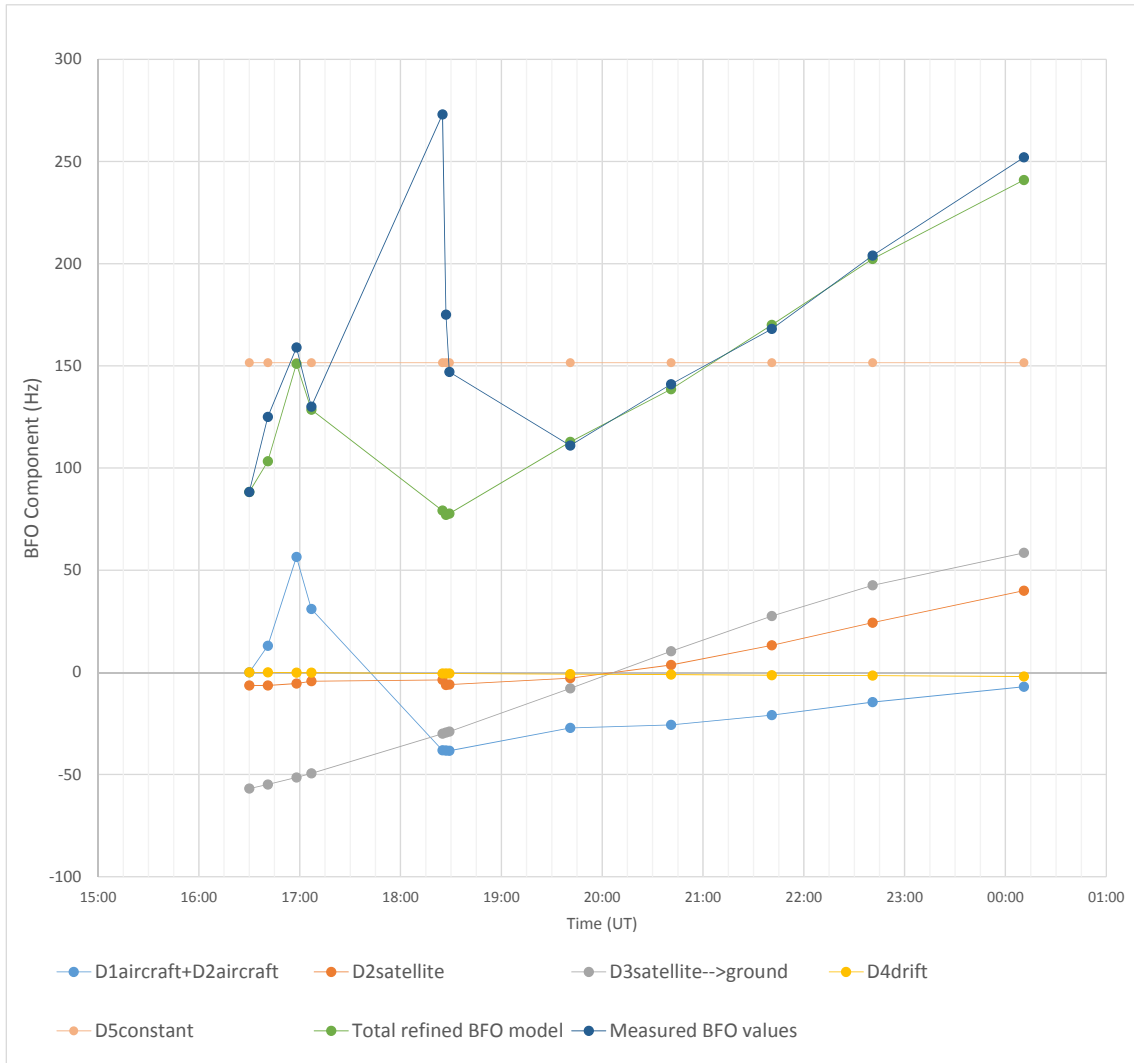


Figure F-1: Components of the Refined BFO model for the three data point example track

### B. Three data point fit

Components of an example fit to the 19:41, 20:41, 21:41 and 22:41 BFO points are shown in figure F-2. In this graph the 19:41UT BFO value is plotted with zero climb rate component.



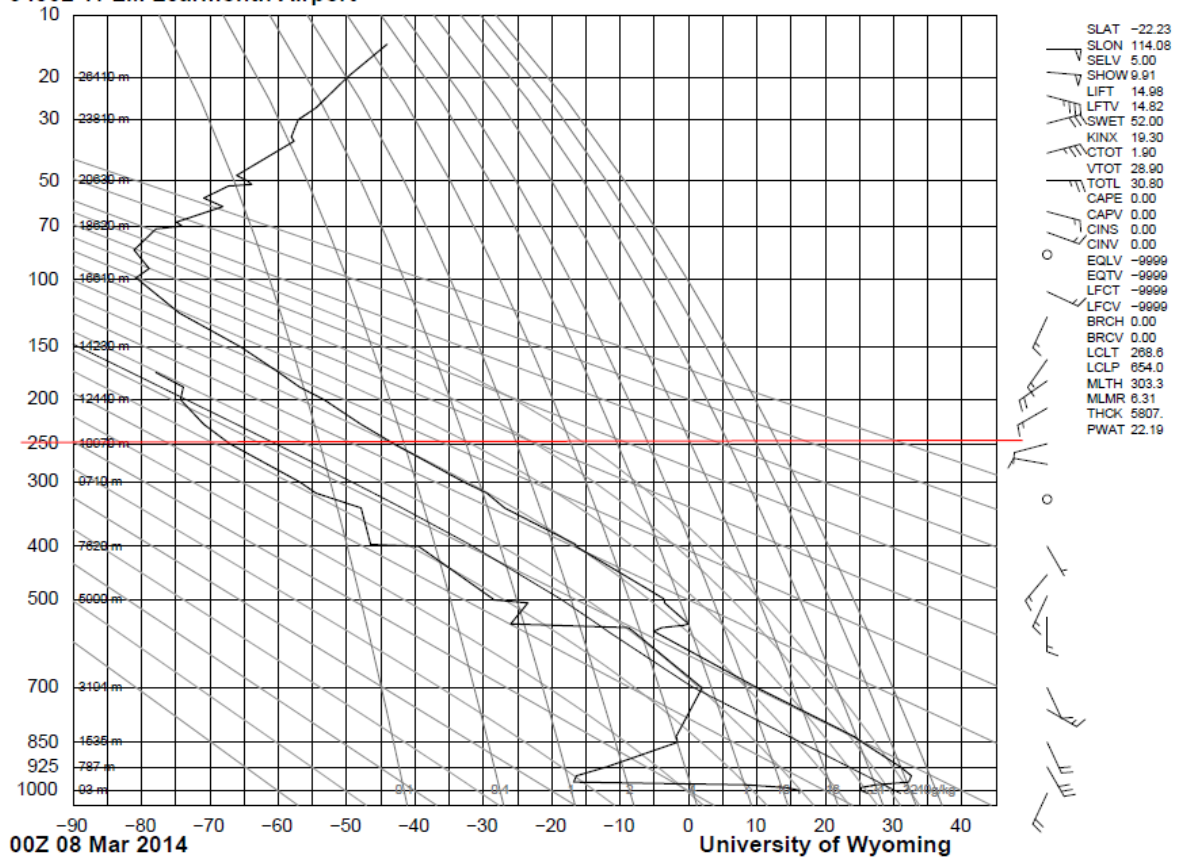
**Figure F-2: Components of the Refined BFO model for the four data point example track**

# Appendix G

## Wind Data

Winds at Learmonth, WA, Australia at 00Z on 8<sup>th</sup> March 2014. The 30,000ft level is indicated.

94302 YPLM Learmonth Airport



**Change record**

Issue	Data	Changes	Notes
1	16/6/14		First issue